1   **CRISPR/Cas with ribonucleoprotein complexes and transiently selected telomere vectors**

2   **allows highly efficient marker-free and multiple genome editing in *Botrytis cinerea***

3

4   **Thomas Leisen[1], Fabian Bietz[1], Janina Werner[1], Alex Wegner[2], Ulrich Schaffrath[2], David Scheuring[1],**

5   **Felix Willmund[1], Andreas Mosbach[3], Gabriel Scalliet[3], Matthias Hahn[1*]**

6

7   [1]University of Kaiserslautern, Department of Biology, Kaiserslautern, Germany

8   [2]RWTH Aachen University, Department of Plant Physiology, 52056 Aachen, Germany

9   [3]Syngenta Crop Protection AG, Stein, Switzerland

10

11   *Corresponding author

12   E-mail: hahn@biologie.uni-kl.de

13

14

15   **Keywords:** *Botrytis cinerea*; necrotrophy; *Magnaporthe oryzae*; ribonucleoprotein complex;

16   CRISPR/Cas9; sgRNA; cotransformation; marker-free editing; botrydial; botcinic acid; Nep1; Nep2;

17   phytotoxin; superoxide dismutase; Sod1; virulence; fungicide resistance; succinate dehydrogenase

18   inhibitor; SdhB; boscalid; fluopyram; pydiflumetofen; telomere vector

19

Abstract

CRISPR/Cas has become the state-of-the-art technology for genetic manipulation in diverse organisms, enabling targeted genetic changes to be performed with unprecedented efficiency. Here we report on the first establishment of robust CRISPR/Cas editing in the important necrotrophic plant pathogen *Botrytis cinerea* based on the introduction of optimized Cas9-sgRNA ribonucleoprotein complexes (RNPs) into protoplasts. Editing yields were further improved by development of a novel strategy that combines RNP delivery with transiently stable telomeres containing vectors, which allowed temporary selection and convenient screening of marker-free editing. We demonstrate that this approach provides vastly superior editing rates compared to existing CRISPR/Cas-based methods in filamentous fungi, including the model plant pathogen *Magnaporthe oryzae*. The high performance of telomere vector-mediated coediting was demonstrated by random mutagenesis of codon 272 of the *sdhB* gene, a major determinant of resistance to succinate dehydrogenase inhibitor (SDHI) fungicides by in bulk replacement of the codon 272 with codons encoding all 20 amino acids. All exchanges were found at similar frequencies in the absence of selection but SDHI selection allowed the identification of novel amino acid substitutions which conferred differential resistance levels towards different SDHI fungicides. The increased efficiency and easy handling of RNP-based cotransformation is expected to greatly facilitate molecular research in *B. cinerea* and other fungi.

Introduction

Botrytis cinerea is a plant pathogenic ascomycete which infects more than a thousand species, triggering gray mold disease which is responsible for over a billion dollars of losses in fruits, vegetables and flowers every year [1]. Due to its worldwide occurrence, great economic importance and non-specific necrotrophic lifestyle, it has been ranked as the second most important plant pathogenic fungus [2]. Control of gray mold often requires repeated treatments with fungicides, in particular under high humidity conditions, but rapid adaption and resistance development of *B. cinerea* has dramatically reduced their efficiency worldwide in many cultures, for example in strawberry fields [3]. After germination of a conidium on the plant surface, the fungus penetrates and invades the host, rapidly killing plant cells by releasing a complex mixture of cell wall degrading enzymes, phytotoxic metabolites and proteins, and by tissue acidification [4, 5]. How host cell death is induced is not fully understood, but the invading hyphae seem to trigger the hypersensitive response, a plant-specific type of apoptosis linked to strong defence reactions [6, 7]. Furthermore, *B. cinerea* releases small RNAs (sRNAs) that can suppress the expression of defence-related genes in its host plants [8]. As a countermeasure, plants also release sRNAs aimed to suppress fungal virulence [9]. To facilitate access to genes or non-coding RNA loci that are important for pathogenesis, a gapless genome sequence of *B. cinerea* has been published recently [10]. Considerable efforts have been made to generate tools for the genetic manipulation of *B. cinerea*. *Agrobacterium*-mediated and protoplast-based transformation have been developed [11–13], and several vectors are available which facilitate the generation of mutants and strains expressing fluorescently tagged proteins for cytological studies[14]. Nevertheless, the generation of mutants remains time-consuming, partly because of the multinuclear nature of *B. cinerea*, which requires several rounds of sub-cultivation to achieve homokaryosis. Furthermore, the generation of multiple knock-out mutants is hampered by the lack of marker recycling systems for serial gene replacements, as described in some filamentous fungi [15].

The application of the clustered regularly interspaced short palindromic repeats (CRISPR)-associated RNA-guided Cas9 endonuclease activity has revolutionized genome editing and greatly facilitated the

3

66   genetic manipulation in a wide range of species [16]. CRISPR/Cas is based on the introduction of double

67   stranded breaks by the Cas9 endonuclease in the genome of an organism. Cas9 targeting occurs by

68   complementary sequences of a single guide RNA (sgRNA), which directs the endonuclease to a genomic

69   target sequence via a 20 bp homology region [17–19]. The sequence requirement, for Cas9 from

70   *Streptococcus pyogenes*, is the presence of the so-called protospacer adjacent motif (PAM), a triplet

71   NGG located immediately 3' of the target[20]. The breaks are then repaired by non-homologous DNA

72   end joining (NHEJ) or, if a repair template (RT) DNA homologous to sequences flanking the break is

73   provided, by homologous recombination (HR), which allows the generation of specific edits in the

74   genome.

75   CRISPR/Cas has been successfully applied in various fungal species using different strategies to deliver

76   Cas9 and the sgRNA [21]. In most cases, codon optimized versions of Cas9 encoding genes were

77   introduced by stable chromosomal integration or transiently via plasmids. To achieve robust

78   expression and efficient nuclear targeting of Cas9, strong fungal promoters, codon-optimized genes

79   and suitable nuclear localization signals fused to the protein are beneficial. Delivery of sgRNA can be

80   achieved either via plasmids or by *in vitro* synthesized sgRNA. More recently, transformation with

81   Cas9-sgRNA ribonucleoprotein (RNP) complexes has been successfully applied in selected fungi [22–

82   24].

83   In this study, we show that CRISPR/Cas-based genome editing is highly efficient in *B. cinerea* when

84   Cas9-sgRNA RNPs are introduced into protoplasts. By using *Bos1* as a selectable marker for gene

85   knockouts, high frequencies of edits via NHEJ and HR were achieved. With RT containing only 60 bp

86   homology flanks, >90% targeting efficiency was observed. Taking advantage of a transiently selectable

87   telomere vector and high cotransformation rates of CRISPR/Cas constructs, a highly efficient marker-

88   free editing strategy was developed, yielding up to thousands of edited transformants per

89   transformation. The power of this approach, which was verified also for *Magnaporthe oryzae*, was

90   demonstrated by random *in vivo* mutagenesis of a resistance-associated codon in a fungicide target

91   gene, and application which was not possible before in filamentous fungi.

4

Results

Establishment and characterization of CRISPR/Cas editing in *B. cinerea*

To achieve strong expression and robust nuclear localization of Cas9, we tested Cas9 constructs with different nuclear localization signals (NLS) using *B. cinerea* transformants expressing a GFP-tagged synthetic Cas9 gene adapted to the low GC content of *B. cinerea* [25]. *B. cinerea* transformants expressing Cas9-GFP with a single C-terminal SV40 T antigen NLS, or with two N- and C-terminal SV40 NLS, both resulted in fluorescence distributed between cytoplasm and nuclei (Fig. 1A-B). In contrast, four tandem copies of SV40 NLS (SV40^{x4}) and a duplicated NLS of the nuclear StuA protein (Stu^{x2}) effectively directed Cas9 into nuclei (Fig. 1C-D).

We next tested which strategy was best suited for Cas9 delivery into *B. cinerea* protoplasts. For stable expression, a construct constitutively expressing Cas9-SV40^{x4} was first integrated into the *niaD* region of the genome. For transient expression, Cas9-GFP-Stu^{x2} cloned into a telomere vector (see below) was transformed into wild type *B. cinereal* [26]. Expression of Cas9 was confirmed by immunoblot analysis (S1 Fig). Alternatively, purified Cas9-Stu^{x2} protein assembled with a sgRNA to a ribonucleoprotein complex (RNP) were used for transformation of wild type *B. cinerea*. CRISPR/Cas activity was evaluated by quantification of error-prone repair via NHEJ, using the *Bos1* gene as a target. *Bos1* encodes a histidine kinase that regulates high osmolarity adaptation via the mitogen activated protein kinase Sak1 [27], which allows for robust positive selection of *Bos1* null mutants which have been shown to be resistant against the fungicides iprodione (Ipr) and fludioxonil (Fld) [28, 29]. With transiently expressed Cas9-GFP-Stu^{x2} and with Cas9-Stu^{x2} RNPs, high numbers of transformants were obtained, whereas stably expressed Cas9-SV40^{x4} yielded significantly less colonies (Fig. 1E). All transformants tested were both Ipr^R and Fld^R, and failed to produce sporulating aerial hyphae. Compared to the wild type (WT), growth of the transformants was more strongly inhibited on media with high osmolarity, and their virulence was strongly reduced when inoculated on tomato leaves (S2 Fig). These phenotypes are consistent with those reported for *Bos1* k.o. mutants [28], and confirmed that *Bos1* was inactivated in the transformants. Due to high, reproducible transformation rates

5

118   obtained, RNP-mediated transformation was used in all subsequent experiments. When recombinant

119   Cas9 protein variants carrying different NLS were compared for their efficiency in RNP-mediated

120   transformation, Stu^{x2} NLS was found to confer the highest *in vivo* editing activities (Fig. 1F).

121   To further characterize CRISPR/Cas-NHEJ editing, Cas9-Stu^{x2}-NLS RNPs with different sgRNAs

122   targeting *Bos1* between codons 344 and 372 were introduced into *B. cinerea* protoplasts. resulted in

123   variable rates of NHEJ-induced mutations (Fig. 2 and S3 Fig). Variable editing frequencies were

124   obtained, which correlated only weakly with *in silico* predictions and with *in vitro* cleavage assays (S3

125   Fig). RNP-induced *Bos1* mutations in Ipr^R transformants were characterized. Most of them showed

126   insertions or deletions of only one or a few nucleotides at the cleavage sites, typical for error-prone

127   NHEJ repair of CRISPR/Cas-induced DNA breaks. With three sgRNAs, a '+T' insertion was predominant,

128   while another sgRNA (Bos1-T7) yielded mostly three types of 9 bp deletions (Fig. 2). Insertions >1bp

129   where found in only 19% of the transformants analyzed. Among 14 insertions of 15-164 bp, three

130   contained *Bos1* DNA derived from sequences close to the sgRNA target sites, and one contained

131   mitochondrial DNA (S4 Fig). The majority of insertions were derived from the scaffold used for sgRNA

132   synthesis, which had apparently resisted the DNase treatment. Several more complex insertions were

133   observed that involved amplification of neighboring *Bos1* sequences (S4 Fig). Taken together, our

134   results show that with selected sgRNAs, error-prone NHEJ-mediated repair in *B. cinerea* results in

135   remarkably uniform mutation patterns.

136

137   **Targeted CRISPR/Cas-mediated editing**

138   To generate targeted *B. cinerea* insertion mutants, and to compare NHEJ- and HR-editing frequencies,

139   a fenhexamid resistance cassette (Fen^R) [30] flanked by 1 kb *Bos1* sequences was delivered as a repair

140   template (RT) in addition to the RNP targeting *Bos1* into protoplasts. Transformants were selected for

141   Fen^R or Ipr^R. Regardless whether the RT was provided as circular plasmid or as PCR product,

142   transformation rates were lower with selection for Fen^R than for Ipr^R. Almost all Fen^R transformants

143   were also Ipr^R, indicating highly efficient HR-mediated integration of the Fen^R cassette into *Bos1*. In

144   contrast, only 22-39% of Ipr^R transformants were Fen^R, indicating a 2.5 to 5-fold higher frequency of

145   NHEJ compared to HR in this experiment (S5 Fig).

146   Conventional gene targeting in filamentous fungi requires resistance cassettes with ≥0.5-1 kb

147   flanking homology regions. A major advantage of HR using CRISPR/Cas is that dsDNA repair can also

148   be achieved using short RT homology flanks [23, 31–33]. To test this for *B. cinerea*, Fen^R cassettes with

149   *Bos1* homology flanks adjacent to the PAM sequence, ranging from 0 to 60 bp, were generated as RT.

150   When delivered as Cas9-RNPs, the numbers of Fen^R transformants increased with increasing flank

151   sizes, reaching highest values with 60 bp flanks (Fig. 3A and 3B). All Fen^R transformants tested were

152   Ipr^R, indicating correct targeting of *Bos1*. Remarkably, even 66% of the transformants obtained with a

153   Fen^R cassette lacking homology flanks were also Ipr^R. Sequencing confirmed that the cassette had

154   integrated via NHEJ into the cleavage site in *Bos1*. When the Fen^R cassettes were delivered without

155   RNP, only few Fen^R transformants were obtained, and none of them were Ipr^R, indicating integrations

156   outside *Bos1* (Fig. 3B). When the 60 bp flanks of the RT were separated by 1 kb each from the PAM site

157   to generate a *Bos1* deletion instead of an insertion, similar transformation efficiencies were obtained

158   (Fig. 3C and 3D). Thus, CRISPR/Cas allows the use of short homology flanks in a flexible way for highly

159   efficient gene targeting.

160   To exploit the efficiency of CRISPR/Cas, co-targeting of two genes encoding key enzymes for

161   biosynthesis of the phytotoxins botrydial (*bot2*) and botcinic acid (*boa6*) was tested. The role of these

162   toxins for *B. cinerea* is not yet completely clear. Whereas single *bot2* and *boa6* knockout mutants did

163   not reveal a decreased pathogenicity, double mutants were found to be impaired in growth and

164   virulence [34]. Cas9-RNPs and RTs with 60 bp flanks targeting *bot2* (using a Fen^R cassette) and *boa6*

165   (using a cyprodinil (Cyp^R) cassette) were generated. In two transformations, 39 and 47 Fen^R colonies,

166   and 16 and 14 Cyp^R colonies, respectively, were obtained (S6A Fig). Of 70 Fen^R transformants tested,

167   49 were Cyp^R, indicating successful coediting. PCR-based DNA analysis of 20 Fen^R Cyp^R transformants

168   revealed 15 transformants as *boa6* k.o., four as *bot2* k.o., and three as *boa6bot2* double k.o., two of

169   which could be purified to homokaryosis (S6B Fig). Thus, double knock-outs can be obtained with Cas-

170 RNPs with high frequency. Phenotypical characterization of the double mutants revealed no significant

171 differences to the WT in their vegetative growth and infection (S6C and S6D Fig). This indicated that

172 the phytotoxins botrydial and botcinic acid are not important for *B. cinerea* to infect tomato leaves.

173

174 **Resistance marker shuttling, a simple strategy for marker-free editing**

175 To generate precise and multiple changes in the genome, marker-free editing is required. Two marker-

176 free mutagenesis strategies were developed, both exploiting the high efficiency of cotransformation,

177 namely that two or more DNA constructs are taken up by fungal cells with much higher frequencies

178 than expected from single transformation rates. The first strategy, called resistance marker shuttling,

179 is based on the integration of an RT into a non-essential genomic locus in exchange for an existing

180 resistance cassette with identical promoter and terminator sequences which serve as homology flanks.

181 To test for marker exchange, a *B. cinerea* strain carrying a nourseothricin (Nat^R) cassette in the *xyn11A*

182 locus [35] was transformed with Cas9-RNP and a Fen^R RT which shared the promoter (*PtrpC*) and the

183 terminator (*TniaD*) sequences with the targeted *nat1* gene as homology flanks (Fig. 4A).

184 Transformations resulted in several hundred Fen^R colonies, and the majority of them had lost Nat^R as

185 expected for a marker exchange. When *Bos1*-RNP was cotransformed, similar numbers of Fen^R

186 transformants were obtained, and 56-74% of them were also Ipr^R, demonstrating a high rate of NHEJ

187 coediting. No marker exchange was observed when the Fen^R RT was transformed without Cas9-RNP

188 as negative control (Fig. 4B). To test the stability of both resistance markers in the Fen^R Ipr^R double

189 transformants, each ten of them were transferred three times to ME agar plates containing only Fen

190 or Ipr. All transformants treated this way retained the non-selected resistance, indicating that

191 coediting had occurred in the same nuclei of the transformed protoplasts. The resulting transformants

192 could be used for another round of marker shuttling, now targeting the Fen^R resistance cassette.

Use of transiently selected telomere vectors for completely marker-free coediting

Previous studies have shown that plasmids containing a pair of telomeres (pTEL) can be efficiently transformed into filamentous fungi and replicate there autonomously as centromere-free minichromosomes, but are rapidly lost in the absence of selective pressure [26]. Based on these properties, a pTEL-mediated strategy for marker-free CRISPR/Cas coediting was developed, involving the following steps (Fig. 5A and 5B): i) cotransformation of pTEL and Cas9-RNP (with or without RT) into *B. cinerea*; ii) selection for pTEL-encoded resistance; iii) identification of transformants with desired coediting events; iv) purification of the transformants by transfers on selective media until homokaryosis is confirmed; v) elimination of pTEL by transfers on nonselective media. This strategy was tested first with pTEL-Fen and Cas9-RNP targeting *Bos1* to generate k.o. mutants via NHEJ. Compared to high transformation rates obtained with pTEL-Fen alone, only few Fen^R colonies were obtained with 0.5-2 µg pTEL-Fen added together with Cas9-RNP to the protoplasts. The suppression of pTEL-Fen transformation by Cas9-RNP was largely overcome by increasing the amount of pTEL-Fen in the transformation mixture up to 10 µg (Fig. 5C). When Fen^R transformants were transferred to Ipr containing medium, 25-53% (average 40.0 ± 11.2%) of them were Ipr^R, which demonstrated a high rate of coediting. After two transfers on nonselective medium, 22 of 26 Ipr^R transformants were Fen^S, confirming the expected loss of pTEL-Fen. Few Ipr^R transformants remained Fen^R after further passages, indicating integration of pTEL-Fen into the genome. In the next cotransformation experiment with pTEL-Fen, *sod1* encoding the major copper/zinc superoxide dismutase was targeted to generate a *sod1-GFP* knock-in fusion (Fig. 5D to 5G). Sod1 has been shown to be involved in oxidative stress tolerance and virulence of *B. cinerea* [36]. Several thousand Fen^R transformants were obtained in single experiments (Fig 5D). Microscopic evaluation revealed GFP fluorescence in 65.3% of the transformants resulting from coediting. Fluorescence was observed in the cytoplasm and in strongly fluorescent punctate structures tentatively identified as peroxisomes (Fig. 5E). For SOD1 of rat, an orthologue of the fungal Sod1, a localization similar to *B. cinerea* was found in the cytoplasm and in peroxisomes, due to its binding to peroxisomal protein CCS [37]. The functionality of the Sod1-GFP fusion protein

9

219   was confirmed by staining for SOD activity after native gel electrophoresis of protein extracts (Fig. 5F)

220   and by immunoblotting using GFP antibodies (Fig. 5G). Furthermore, pTEL-mediated coediting was

221   shown to be useful for marker-free mutagenesis of *nep1* and *nep2*, two genes encoding necrosis and

222   ethylene-inducing proteins [38]. With single targeting, >1,000 Fen^R transformants were obtained, and

223   17-23% of these contained *nep1* or *nep2* deletions, respectively, as confirmed by PCR. Co-targeting of

224   *nep1* and *nep2* resulted in 230 transformants. Of these, 12.9% contained a *nep1* deletion and 10% a

225   *nep2* deletion (S7 Fig), but no double transformants were detected.

226

227   **Telomere vector-mediated marker-free coediting also works efficiently in *Magnaporthe oryzae***

228   The rice blast fungus *M. oryzae* is of great economic importance and considered as the prime model

229   pathogenic fungus [2]. It is a hemibiotroph and well-known for its ability to develop enormous turgor

230   pressure in appressoria facilitating penetration of host cells [39]. Recently, protoplast transformation

231   with CRISPR/Cas using RNP has been successfully applied for this fungus [23]. Marker-free editing was

232   also demonstrated, however, rates of non-selected coediting events ranged only from 0.5 to 1.2%.

233   Aiming to improve this rate, we first confirmed the efficacy of CRISPR/Cas with Cas9-RNP. *M. oryzae*

234   strain Guy11 or Guy11ku80 (a NHEJ deficient mutant) protoplasts were transformed with Cas9-SV40^{x4}

235   complexed with sgRNA *MoALB1* and a Hyg^R RT with 50 bp homology flanks. *MoALB1* encodes a

236   polyketide synthase required for melanin biosynthesis and *alb1* mutants are easily selectable due to

237   whitish mycelium. Depending on the amount of RT DNA and strain used, 67 to 91% of Hyg^R

238   transformants had white mycelium, indicating successful inactivation of *MoALB1* (S8 Fig).

239   Next, we tested the suitability of the pTEL-based marker-free approach for *M. oryzae*. After

240   establishing selection for Fen^R, using 30 ppm fenhexamid, pTEL-Fen was transformed yielding up to

241   1,000 transformants per μg DNA (S1 Table). Subsequently, pTEL-Fen was cotransformed together with

242   Cas9-sgRNA RNP targeting *MoALB1*. Among Fen^R transformants, 36-49% displayed white colonies in

243   Guy11, indicating a high rate of co-editing (Fig. 6). By contrast, the rate of cotransformation in

244   Guy11ku80 was much lower. Sequencing of *MoALB1* in three of the white Fen^R colonies of Guy11

10

245   revealed the presence of single base pair deletions at the cleaving site, leading to frameshifts. After

246   two passages on non-selective medium, 12 out of 15 albino mutants were Fen[S], as predicted from the

247   instability of pTEL-Fen. To show that coediting with insertion of a RT into a specific locus is possible as

248   well, pTEL-Fen, Cas9-RNP targeting the *MoPIT* gene MGG_01557 and a Hyg[R] cassette with 50 bp flanks

249   were cotransformed into *M. oryzae* protoplasts (S9 Fig). While 23 out of 72 Fen[R] transformants were

250   Hyg[R], *MoPIT* knockouts were detected in five of these, representing a coediting rate via HR of 7%.

251   However, no coediting was observed in *M. oryzae* Guy11ku80.

252

253   **Randomized amino acid editing of a fungicide resistance codon and *in vivo* selection**

254   Succinate dehydrogenase inhibitor (SDHI) fungicides have emerged as the fastest increasing class of

255   fungicides for the control of plant diseases in recent years [40]. Target site mutations leading to

256   resistance against SDHI have been described in *B. cinerea* and other fungi. Most of them are located

257   in *sdhB* encoding the B-subunit of the succinate dehydrogenase enzyme (complex II), an essential

258   component of mitochondrial respiration. In *B. cinerea* populations from SDHI-treated fields, *sdhB*

259   mutations leading to H272R, H272Y, H272L, and H272V amino acid exchanges have been found [41].

260   While all of them confer resistance to boscalid (Bos), only H272L and H272V mutations also confer

261   resistance to another SDHI, fluopyram (Flu) [40, 42]. To analyze the effects of all possible exchanges in

262   codon 272 for SdhB function and resistance against SDHIs, pTEL-mediated coediting was performed to

263   target *sdhB* with a RT mixture encoding all 20 amino acids in codon 272 (Fig. 7A). Several thousand

264   colonies were obtained per transformation. Estimations based on PCR analysis of single transformants

265   revealed coediting frequencies between 12.5 and 41% (S2 Table). The distribution of codons in position

266   272 was determined from pooled conidia of ≥6,000 Fen[R] transformants per assay by bulked DNA

267   isolation, followed by deep sequencing. Aliquots of pooled transformant conidia were cultivated for

268   three days in liquid medium containing discriminatory concentrations of Bos, Flu, or the new SDHI

269   fungicide pydiflumetofen (Pyd) [43], to select transformants with SDHI resistance. DNA of these

270   cultures was isolated and sequenced as above. Among the edited transformants grown on SH+Fen

11

271   plates, all 20 codons were represented at similar frequencies (Fig. 7B). Because in this procedure edited

272   cells may still carry a WT copy of *sdhB* (heterokaryons), we cannot conclude yet that they all

273   maintained full enzyme function. However, our results demonstrate that all H272 amino acids variants

274   yield functional SdhB proteins that are not intrinsically toxic since they all similarly maintained growth

275   and sporulation. Cultivation of the Fen^R transformants in SDHI-containing media followed by

276   quantification of the alleles enabled an unbiased assessment of amino acid exchanges conferring

277   resistance. Most conspicuous resistance mutations were H272K/V/L/R/Y for Bos, H272N/L/V/I for Flu,

278   and H272V/L for the new SDHI Pyd (Fig. 7C-7E). Transformants with 17 different exchanges in codon

279   272 were isolated, purified to homokaryosis, and tested for sensitivity to the three SDHI (Fig. 7F).

280   Overall, the EC_{50} values correlated well with their prevalence in the SDHI selected populations

281   described above (Fig. 7c-d). Remarkably, 12 amino acids conferred high levels of resistance to boscalid

282   (EC_{50} values >2mg l^{-1}) (Fig. 7C). In contrast, only four amino acids conferred similarly high resistance

283   levels to Flu, but five amino acids caused up to 30-fold hypersensitivity compared to WT (Fig. 7D). Pyd

284   was about ten times more active than Bos and Flu against *B. cinerea* WT, and four amino acids

285   conferred EC_{50} values >0.2mg l^{-1} (Fig. 7F). Only the three aliphatic amino acids leucine, valine and

286   isoleucine provided high or intermediate resistance to all three SDHI. Remarkably, highest resistance

287   levels were observed with isoleucine, which has never been found in resistant field isolates. Growth

288   on selective agar media illustrated the high proportion of Bos^R mutants, and the lower number of

289   mutants resistant to Flu and Pyd (Fig. 7G). Growth on rich medium and on a nutrient-limited medium

290   with different carbon sources did not reveal significant differences between the 17 edited strains (S10

291   Fig), indicating no major effects of the amino acids on the fitness of the mutants during vegetative

292   growth.

Discussion

Within a short time, CRISPR/Cas genome editing has been used for the genetic manipulation of a wide range of organisms, offering new perspectives in functional genomics. In fungi, advanced CRISPR/Cas systems have been mainly established for *Aspergillus* spp. [31, 44, 45] and *Ustilago maydis* [21, 46]. They take advantage of autonomously replicating circular plasmids, namely the *Aspergillus*-derived AMA1 plasmid and pMS7 in *U. maydis*, for the delivery of Cas9 and sgRNA. AMA1 has also been used in other fungi, including the plant pathogens *Alternaria alternata* [47] and *Fusarium fujikuroi* [48]. However, this plasmid displays only low transformation rates in *B. cinerea* (S. Fillinger, personal communication). Alternatively, a non-integrating vector with human telomeres [26, 49] has been developed in this study as a tool for coediting in *B. cinerea* and *M. oryzae*.

This is the first report of powerful use of CRISPR/Cas in *B. cinerea*. A crucial step was the generation of a fully functional, nuclear targeted Cas9. SV40 NLS has been used frequently [21], but efficient nuclear targeting of Cas9-GFP-NLS has been confirmed only in some fungi [24, 50] or optimal activity experimentally verified [48]. In *B. cinerea*, efficient Cas9 nuclear targeting was achieved with C-terminal tandem arrays of either SV40 (4x) and *stuA* (2x) NLS sequences. In most fungi, CRISPR/Cas activity was detected in pilot studies by targeting genes for the biosynthesis of melanin [23, 44]. Following the strategy reported for *Fusarium graminearum* [51], *Bos1* was established as an effective selectable marker for NHEJ- and HR-mediated mutagenesis (Fig. 1 and 3). Introduction of Cas9-sgRNA RNPs with or without a donor template yielded hundreds to thousands of edited *B. cinerea* transformants. So far, similar approaches have been rather rarely used for CRISPR/Cas genome editing in fungi [22–24]. An advantage of the use of RNP over endogenous Cas9 and sgRNA expression is the reduced probability of potential off-target mutagenic activities of Cas9, because of its limited stability in cells [52]. Furthermore, sgRNAs synthesis is performed quickly and does not require any cloning steps.

A total of 153 NHEJ repair events in the *Bos1* gene were analyzed, which is the largest number reported for filamentous fungi. Most changes were 1-2 bp indels, and for three sgRNAs inducing a T↓N

319 cleavage by Cas9, a (+T) insertion was the dominating mutation. Although all these mutations were

320 biased by the selection for loss of *Bos1* function (Ipr^R), these data are in line with systematic studies of

321 CRISPR/Cas-NHEJ mutations in human cells and yeast [53, 54] which often resulted in +1 bp insertions

322 at the Cas9-RNP cleavage site. This rather reproducible NHEJ repair in *B. cinerea* could be exploited to

323 introduce predictable frameshift mutations even without RT. Furthermore, we demonstrate that RTs

324 with 60 bp homology flanks worked efficiently in *B. cinerea*, yielding >90% targeted integrations

325 (Fig. 3). Such short flanks can be attached to a resistance cassette of choice using long PCR primers,

326 avoiding time-consuming cloning or amplification steps which were previously required to generate

327 the long homology flanks for conventional targeted integration.

328 In *B. cinerea*, cotransformation occurred with rates of up to >60%, both for different combinations

329 of CRISPR/Cas-induced integrations (HR/HR or HR/NHEJ) and for telomere vector uptake and

330 CRISPR/Cas events (HR or NHEJ). Cotransformation rates were found to increase with higher DNA

331 concentrations, consistent with early reports for fungi [55]. Two novel strategies have been established

332 for marker-free coediting. Resistance marker shuttling at a non-essential locus in combination with

333 non-selected CRISPR/Cas events allows repeated genomic edits. High frequencies (65.3%) of marker

334 replacement were observed in the transformants, and this approach is also applicable for other

335 organisms. A prerequisite for successful coediting in multinuclear fungi such as *B. cinerea* is the

336 generation of homokaryons, which requires integration of different DNA fragments into the same

337 nuclei. In most transformants analyzed this was found to be the case, similar to previous reports for

338 *Neurospora crassa* [56].

339 The most powerful approach for marker-free editing is cotransformation of pTEL vector and CRISPR

340 constructs. Its effectiveness depends on i) high transformation efficiency of pTEL which provides the

341 selection, ii) high rates of cotransformation/coediting of pTEL and CRISPR components, iii) highly

342 efficient HR, and iv) elimination of pTEL after identification of the desired editing event(s), yielding

343 edited strains without any other genomic alterations. With this approach, we reproducibly obtained

344 hundreds to thousands of transformants, and up to >50% of them were marker-free edits. Similar

14

345 results were obtained for NHEJ- and HR-induced edits, as shown for NHEJ-mediated mutagenesis of

346 *Bos1*, RT-mediated knock-in attachment of a GFP tag to *sod1*, and deletion of *nep1* or *nep2*.

347 Importantly, we could show that the pTEL strategy is also applicable for coediting approaches in other

348 filamentous fungi. pTEL-Fen transformed *M. oryzae* with equal efficiency as *B. cinerea*, and coediting

349 frequencies were 36-49% for NHEJ, and 7% for RT-mediated HR. These values clearly exceed coediting

350 rates previously reported with integrative selected markers [23]. The lower rate of coediting in *M.*

351 *oryzae* with HR is probably due to the intrinsically lower efficiency of HR compared to *B. cinerea*. This

352 could be partially compensated by using RT with longer homology flanks. We therefore expect that

353 cotransformation with pTEL vectors will significantly facilitate the establishment of RNP-based

354 CRISPR/Cas coediting in many fungi, and maybe also in non-fungal microbes such as oomycetes.

355 The power of pTEL-mediated marker-free editing was exploited by performing an unbiased directed

356 mutagenesis of codon 272 of *sdhB* encoding the succinate dehydrogenase B subunit, the gene in which

357 most mutations conferring resistance against SDHI fungicides have been observed in *B. cinerea* field

358 isolates [39]. Among sporulating transformants, edited strains with all amino acid substitutions were

359 generated with similar frequencies, compared to only four changes detected in field isolates. Drastic

360 differences were observed for the effects of each amino acid on the sensitivity or resistance to the

361 three SDHI tested, which underlines the importance of the conserved histidine 272 for SDHI binding

362 [57]. The majority of substitutions caused high levels of resistance to Bos, whereas fewer substitutions

363 conferred similar resistance levels to Flu and Pyd. Our results are consistent with the observation that

364 Bos[R] resistant *B. cinerea* field isolates with H272R and H272Y substitutions were sensitive or even

365 hypersensitive to Flu and still controllable by this SDHI [41]. Previously, phenotypic characterization of

366 field isolates and of isogenic H272R, H272Y and H272L strains generated by conventional mutagenesis

367 with simultaneous introduction of a resistance cassette at the *sdhB* target locus indicated that these

368 substitutions caused fitness defects, such as aberrant growth and differentiation and reduced

369 competitiveness [58–60]. Although our analysis of the edited strains did not include enzyme activity

370 assays, their equal distribution upon primary selection and normal growth behavior on different media

15

371 does not support this conclusion. Indeed, this might reflect the great advantage of precise marker-free

372 genome editing in avoiding any modification of neighboring genes or their regulatory sequences by co-

373 introduction of a nearby resistance cassette. Another benefit of our approach is that it allows the

374 analysis of several independent mutants that have been obtained without selection of the target locus.

375 This might obviate the need for tedious complementation experiments to verify the connection

376 between mutations and phenotypes. We further show how selection post-mutagenesis can enable the

377 rapid scanning of mutations conferring resistance to various SDHI fungicides. Since a vast set of target

378 mutations and fungicides can be tested, this new capability is of major relevance for accelerated

379 fungicide design. Interestingly, several substitutions conferring high resistance levels, such as H272I,

380 H272C and H272T have not yet been detected in field populations and suggest that a bias prevented

381 their appearance and propagation in nature. Fungicide resistance mutations are often caused by single

382 nucleotide exchanges, for example the major mutations against most systemic fungicides in *B. cinerea*

383 [3, 61], including the exchanges H272R/Y/L in SdhB [62]. An obvious explanation for their unequal

384 occurrence is their differential effects on fungal fitness, therefore mutations resulting in minimal

385 fitness costs are most likely to occur [63]. Our data, showing similar SDHI resistance and fitness levels

386 caused by hitherto unknown substitutions seem to indicate that fungicide resistance development in

387 field populations is also limited by the number and probability of mutations required to change one

388 codon to another [64].

389   The high yield of telomere vector-mediated coediting in combination with RNP-CRISPR/Cas opens

390 the door to advanced genome editing applications with *B. cinerea* and other fungi, such as large-scale

391 mutagenesis and gene tagging projects. Approaches similar to mutagenesis of *sdhB* codon 272 are now

392 possible for *in vivo* selection and structure-function analysis of proteins, such as those involved in

393 fungicide resistance, host invasion or any other functions of interest.

16

Materials and Methods

Fungi. *Botrytis cinerea* B05.10 was used as WT strain in this study. For demonstration of CRISPR/Cas-assisted marker replacement, a *B. cinerea* B05.10 derivative, containing a Nat^R cassette (*PtrpC-nat-TniaD*) integrated in *xyn11A* [35] was used. Cultivation of *B. cinerea* and infection tests were performed as described [5]. Guy11 was used as *Magnaporthe oryzae* WT strain. A NHEJ-deficient *M. oryzae* mutant, Guy11ku80, was kindly provided by A. Foster.

DNA constructs for transformations. All oligonucleotides used are listed in Supplementary Table 3. Sequences of plasmids marked with * are provided in Supplementary file 1. Derivates of the telomere vector pFAC1 [26] were constructed as following: pFAC1 was digested with BglII/NheI, and the vector fragment ligated with a synthetic linker made by annealing of oligonucleotides pFAC1-del1/pFAC1-del2, resulting in pFB2N*, carrying a hygromycin resistance cassette. For telomere vector-mediated coediting, a truncated version of pFB2N carrying a fenhexamid resistance marker was generated, called pTEL-Fen*. A codon optimized version of the *Streptococcus pyogenes cas9* gene for expression in *B. cinerea*, under the control of *oliC* promoter from *A. nidulans*, was synthesized by Genewiz (South Plainfield, NJ, USA). To generate a stable Cas9 expressing *B. cinerea* strain, a nourseothricin resistance cassette consisting of *A. nidulans trpC* promoter (Ptrpc), *nat* gene and *B. cinerea gluc* terminator (Tgluc) [14] was integrated next to the *cas9* gene, and homology flanks for targeted integration of the construct into *niaD* encoding nitrate reductase were added. For efficient nuclear localization of Cas9, a synthetic sequence encoding four copies of the SV40 T antigen NLS (SV40^{x4}) was C-terminally attached to the *cas9* coding sequence, resulting in pUC-BcCas-SV40x4_nat_niaD*.To test different NLS arrangements for their efficiency to target Cas9 into nuclei of *B. cinerea*, Cas9 was fused to GFP codon-optimized for *B. cinerea* (from pNAH-OGG [14]) and the following NLS sequences C-terminally attached: Single copy SV40, SV40^{x4}, Stu^{x2} (a tandem duplicated NLS of Bcin04g00280 encoding a homologue of the *A. nidulans* nuclear protein StuA [47]), and SV40^{x2} (each one N- and C-terminal SV40). For transient expression of Cas9-GFP, pFB2N was first truncated by digestion with BlpI/SphI, followed by ligation with the annealed oligonucleotides FB108/ FB109, resulting in pFB2N_BlpI_MreI. This plasmid was digested with BlpI/MreI and ligated with fragments containing Cas9-GFP-NLS, resulting in pTEL-BcCas9GFP-NLS-SV40x4* and pTEL-BcCas9GFP-NLS-Stux2*.

To generate a RT with 1 kb *Bos1* homology flanks and a fenhexamid resistance cassette, pBS-KS(-) was digested with EcoRV and combined by Gibson assembly with two adjacent 1 kb *Bos1* homology flanks, using primers TL29 pBS_ol_bos 3.REV/ TL30 pBS_ol_bos 3.FOR and TL31 pBS_ol_bos 1.FOR/ TL32 pBS_ol_bos 1.REV, and a fenhexamid resistance cassette amplified from pNDF-OCT [30] with primers TL33 Fen_ol_bos 2.FOR/TL34 Fen_ol_bos 2.REV. From the resulting plasmid (pBS_Bos1_KO_Fen), *Bos1* RT with short homology flanks were amplified with the following primers: TL37_Fen_fw/ TL38_Fen_rev

17

428   (0 bp); TL65_Bos1_Fen30_fw/ TL66_Bos1_Fen30_rev (30 bp), TL67_Bos1_Fen40_fw/

429   TL68_Bos1_Fen40_rev (40 bp); TL69_Bos1_Fen60_fw/ TL70_Bos1_Fen60_rev (60 bp). A RT with 60 bp

430   *Bos1* homology flanks at 1 kb distance from the cleavage site was amplified from pTel-Fen using

431   primers TL113 60bp Bos1 PD FW/ TL114 60bp Bos1 PD RV. For generation of *boa6* k.o. mutants, a

432   newly designed cyprodinil resistance cassette was used (Leisen et al., unpublished).

433   **Expression of Cas9 protein with *B. cinerea* optimized NLS.** SV40^{x4} and Stu^{x2} NLS were fused to the 3'-

434   terminus of *Streptococcus pyogenes* Cas9 (*E. coli* codon optimized) and cloned into pET24a. The

435   resulting plasmids, pET24a_Cas9-SV40x4-NLS-His* and pET24a_Cas9-Stux2-NLS-His* were used to

436   express these Cas9 derivatives in *E. coli* BL21(DE3) at 20°C in autoinduction medium. Cells were

437   harvested and ca. 10 g of cell paste resuspended in 50 ml extraction buffer (20 mM HEPES, 25 mM

438   imidazole, 500 mM NaCl, 0.5 mM TCEP, pH 8) by stirring for 40 min. Cells were lysed using a Cell

439   Disruptor (Constant Systems Limited, Daventry, UK) at 20,000 psi, and the lysate clarified by

440   centrifugation at 20,000 rpm in a fixed-angle rotor for 30 min, 4°C. The lysate was applied to a 5 ml

441   HisTrap FF column equilibrated in extraction buffer. Bound protein was eluted with 3.5 column

442   volumes of elution buffer (20 mM HEPES, 500 mM imidazole, 500 mM NaCl, pH8, 0.5 mM TCEP). The

443   eluate was loaded onto a GE 26/60 S200 SEC column equilibrated in 20 mM HEPES, pH8, 0.5 mM TCEP.

444   Fractions containing the target protein were pooled and 20 % (v/v) glycerol was added. The solution

445   was concentrated using a 10 kDa Vivaspin column. Aliquots were frozen in liquid nitrogen and stored

446   at -80°C until use. Functionality of *in vitro* assembled Cas9-sgRNA complexes was tested by *in vitro*

447   cleavage of target DNA as described [65].

448   **Synthesis of sgRNA and RNP formation.** Selection of appropriate sgRNAs was carried out with the help

449   of the sgRNA design tool of the Broad Institute (https://portals.broadinstitute.org/gpp/public/analysis-

450   tools/sgrna-design). Oligonucleotides for synthesis of sgRNAs are listed in Supplementary Table 3. DNA

451   template preparation was performed by annealing 10 µmol each of constant sgRNA oligonucleotide

452   (TL147_gRNA rev) and protospacer specific oligonucleotide in 10 µl in a thermocycler (95°C for 5 min,

453   from 95°C to 85°C at 2°C sec^{-1}, from 85°C to 25°C at 0.1°C^{-1}), followed by fill-in with T4 DNA polymerase

454   (New England Biolabs, Beverly, MA, USA), by adding to the annealing mix 2.5 µl 10 mM dNTPs, 2µl 10x

455   NEB buffer 2.1 (50 mM NaCl, 10 mM Tris-HCl, 10 mM MgCl$_2$, 100 µg ml^{-1} BSA, pH 7.9), 5 µl water and

456   0.5 µl enzyme, and incubation for 20 min at 12°C and column purification. Subsequently, sgRNA

457   synthesis was performed using the HiScribe™ T7 High Yield RNA Synthesis Kit (NEB), and purified using

458   the RNA Clean & Concentrator-25 kit (Zymo Research, Orange, CA, USA). Cas9-NLS, containing N- and

459   C-terminal SV40 NLS, was purchased from NEB. For RNP formation, 6 µg Cas9 was incubated in

460   cleavage buffer (20mM HEPES, pH 7.5, 100 mM KCl, 5% glycerol, 1 mM dithiothreitol, 0.5 mM EDTA,

461   pH 8.0, 2 mM MgCl$_2$) with 2 µg sgRNA for 30 min at 37°C.

18

462 **Transformation of *B. cinerea*.** Transformation was performed based on a published protocol[5] as

463 following: 10^8 conidia harvested from sporulating malt extract (ME: 10 g/l malt extract, 4 g/l glucose,

464 4 g/l yeast extract, pH 5.5) agar plates were added to 100 ml ME medium and shaken at 180 rpm for

465 ca. 18 h (20-22°C) in a 250 ml flask. The germlings was transferred into 50 ml conical tubes and

466 centrifuged (8 min, 1,000 g) in a swing-out rotor. The combined pellets (fresh weight should be >3 g)

467 were resuspended and washed two times with 40 ml KCl buffer (0.6 M KCl, 100 mM sodium phosphate

468 pH 5.8; centrifugation for 5 min, 1,000 g), and the germlings resuspended in 20 ml KCl buffer containing

469 1% Glucanex (Sigma Aldrich, St Louis, MO, USA; L1412) and 0.1 % Yatalase (Takara, T017), and

470 incubated on a 3D rotary shaker at 60 rpm for 60-90 min at 28°C until ca. 10^8 protoplasts had been

471 formed. Protoplasts were filtered through a sterile nylon mesh (30 µm pore size) into a 50 ml conical

472 tube containing 10 ml ice-cold TMS buffer (1 M sorbitol, 10 mM MOPS, pH 6.3). After addition of

473 another 30-40 ml ice-cold TMS buffer, the suspension was centrifuged (5 min, 1500 g, 4°C), and the

474 protoplast pellet resuspended in 1-2 ml TMSC buffer (TMS + 50 mM $CaCl_2$, 0°C, dependent on the

475 desired protoplast concentration. To 0.5 x10^6 to 2x10^7 protoplasts in 100 µl TMSC, the Cas9/sgRNA

476 ribonucleoprotein (RNP) complex (6 µg Cas9, 2 µg sgRNA; pre-complexed for 30 min at 37°C) and up

477 to 10 µg donor template DNA were added in 60 µl Tris-$CaCl_2$ buffer (10 mM Tris-HCl, 1 mM EDTA, 40

478 mM $CaCl_2$, pH 6.3). After 5 min incubation on ice, 160 µl of PEG solution (0.6 g ml^{-1} PEG 3350, 1 M

479 sorbitol, 10 mM MOPS, pH 6.3; pre-heated to 60°C, mixed, and allowed to cool down to 30-40°C) was

480 added, mixed gently, and incubated for 20 min at room temperature. 680 µl of TMSC buffer was added,

481 the sample was centrifuged (5 min, 1,500 g in a swing-out rotor), the supernatant removed, and

482 protoplasts suspended in 200 µl TMSC. Protoplasts were transferred into 50 ml liquid (42°C) SH agar

483 (0.6 M sucrose, 5 mM Tris-HCl pH 6.5, 1 mM $(NH_4)H_2PO_4$, 9 g l^{-1} bacto agar, Difco) and poured into two

484 Petri dishes. For transformation with pTEL-Fen, up to 10 µg plasmid DNA was used. For selection of

485 transformants, 30 mg l^{-1} nourseothricin (Nat), 1 mg l^{-1} fenhexamid (Fen), 4 mg l^{-1} iprodione (Ipr), or

486 mg l^{-1} fludioxonil (Fld) were added. Positive colonies were transferred onto ME agar plates or onto

487 plates containing the same concentrations of selective agents. Transformants were subcultured on

488 selective media and purified by three to five rounds of single spore isolation. Genomic DNA was

489 isolated as described previously [66].

490 **Transformation of *M oryzae*.** Three-day old cultures of *M. oryzae* Guy11 or the Guy11ku80 deletion

491 mutant, grown in 150 ml liquid complete media at 25°C and 100 rpm, were used for generation of

492 protoplasts. The mycelia were filtered and digested with Glucanex as described above [67]. Protoplasts

493 purification was done according to the protocol for *B. cinerea*. After washing with TMS buffer,

494 protoplasts were suspended in TMSC buffer and adjusted to 1.5x10^8 protoplasts per ml. For

495 transformation, 120 µl aliquots of a protoplast suspension were mixed with the RT DNA and pre-

496 incubated RNPs (Cas9-SV40^{x4}) dissolved in 60 µl Tris-$CaCl_2$ buffer. Then 180 µl 60% PEG 3350 were

19

497 added, and the protoplast suspension was poured into CM agar containing 1.2 M sucrose for osmotic

498 stabilization. After 24 h an upper layer containing 500 mg l^{-1} hygromycin (Hyg) or 30 mg l^{-1} Fen was

499 poured over the agar containing the protoplasts. After 7-10 days, mutants were transferred to

500 selection plates for further selection. RT (containing *gpd3* promotor, *hph* and *tubB* terminator) with

501 50 bp of homology flanks was amplified using primers MH-Alb F&R for targeting *MoAlb1*, and MH-Pit

502 F&R for targeting *MoPIT*. For sgRNA synthesis, primers sgRNA_Alb1 and sgRNA_Pit were used.

503 Transformants were verified using primers SeqPit F/R, SeqAlb F/R and MoPit FL F/R.

504 **Generation and *in vivo* selection of *sdhB* codon 272 edited strains.** To be used as mixed RT for

505 randomized editing, twenty 500 bp *sdhB* fragments differing in codon 272 (listed in Supplementary

506 Table 4) were synthesized by Twist Bioscience (San Francisco, U.S.A.) and pool-amplified with primers

507 TL148_ SDHB_RT_F/ TL149_ SDHB_RT_R. Illumina deep sequencing was performed to verify equal

508 representation of each fragment (±7.5%). For PCR-based identification of edited transformants, silent

509 mutations were introduced into the 500 bp fragments which converted an XhoI to an XbaI site (codons

510 278/279), and allowed differentiation between WT and edited sequences (Fig. 7a). To isolate the DNA

511 of *sdhB* codon 272-edited transformants for sequencing, sporulation was induced on the primary

512 transformation plates. For this, three days after transformation, the SH+Fen agar containing

513 embedded transformants was overlaid with 0.1 volumes of 5x concentrated ME medium. After

514 another 5-7 days, transformant conidia were harvested from densely sporulating plates. To improve

515 the recovery of transformants, the agar discs were inverted, placed onto fresh ME (1 mg l^{-1} Fen) agar

516 plates, and incubated again for 5-7 days until sporulation. Conidia harvested from one transformation

517 were combined and used for DNA isolation. For sequence analysis of bulked transformants selected

518 for resistance to SDHI, 4×10^5 conidia of Fen^R transformants were inoculated in standard Petri dishes

519 with 18 ml YBA medium (1% yeast extract, 20 g l^{-1} sodium acetate[68]) containing boscalid (0.25 mg l^{-1};

520 ^{1}; BASF, Ludwigshafen, Germany), fluopyram (0.3 mg l^{-1}; Bayer Crop Science, Monheim, Germany), or

521 pydiflumetofen (0.015 mg l^{-1}; Syngenta Crop Protection, Stein, Switzerland) in concentrations

522 inhibitory for *B. cinerea* WT strain B05.10. After 72 h incubation at 20°C, conidia and germlings were

523 harvested and used for DNA isolation [66] and sequencing (see below).

524 To isolate *sdhB* edited strains with defined codon 272 replacements, individual Fen^R transformants

525 were purified by several transfers on ME+Fen (1 mg l^{-1}), YBA+Bos (1 mg l^{-1}), or YBA+Flu (2.5 mg l^{-1}) agar

526 media. Total DNA of these isolates was amplified using primers TL151_SDHB_OS_F/

527 TL152_SDHB_OS_R, and the 741 bp products digested with either XbaI or XhoI to test whether they

528 were edited or WT. Edited isolates were sequenced using primer TL148_ SDHB_RT_F or TL149_

529 SDHB_RT_R.

530   **Sequencing.** For deep sequencing of edited transformants, bulked *B. cinerea* DNA was first amplified

531   in 20 µl total volume, with 2 µl DNA, 10 pM of primers sdhb_F1/ sdhb_R1, 1x MyTaq^{TM} buffer, and 1

532   Unit MyTaq^{TM} (Bioline; Meridian Bioscience Inc., London, UK) by incubation for 2 min at 96°C, followed

533   by 20 cycles of 15sec 96°C, 30sec 60°C, 90sec 70°C. Nested PCR was performed in 20 µl total volume,

534   using 2 µl of the first round PCR, under the same conditions as above, but with 15 cycles only. PCR

535   products were purified with AmpureXP beads (Thermo Fisher Scientific, Bremen, Germany). About 100

536   ng of each purified PCR product was used to construct Illumina libraries using the Ovation Rapid DR

537   Multiplex System 1-96 (NuGen Technologies, San Carlos, CA, USA). Illumina libraries were pooled and

538   size selected by preparative gel electrophoresis. Sequencing (3 million reads per sample) was

539   performed by LGC Genomics (Berlin, Germany) on an Illumina NextSeq 550 instrument with v2

540   chemistry in 2x150 bp read mode. Libraries were demultiplexed using Illumina's bcl2fastq 2.17.1.14

541   software. Sequencing adapter sequences were removed from the 3' end of reads with cutadapt

542   (https://cutadapt.readthedocs.io/en/stable/) discarding reads shorter than 20 bp. All read pairs were

543   filtered for valid primer combinations and reverse-complemented so that R1 corresponds to the

544   forward primer and R2 to the reverse primer. Actual primer sequences were removed for downstream

545   processing. Reads were quality-filtered by LGC proprietary software, removing all reads with an

546   average Phred score below 30, and all reads containing more than 1 undetermined base

547   (N). Subsequently, all read pairs were overlap-combined using BBMerge 34.48 from the BBMap

548   package (https://jgi.doe.gov/data-and-tools/bbtools/bb-tools-user-guide/bbmerge-guide/). Mutated

549   positions were identified by a custom shell script, filtering for sequences containing the motifs

550   immediately before and after thse mutated triplet (TTTGTACAGATGT and ACTATTCTCAACTG,

551   respectively). The sequence content between these motifs were extracted and counts for the detected

552   sequences summarized for each sequencing library.

553   **Fungicide susceptibility test.** Isolates with defined edits in codon 272 were tested for radial growth on

554   YSS agar with 50 mM each of either glucose, malate, acetate or succinate [59], and for their sensitivities

555   to SDHIs. Susceptibility to Bos (BASF), Flu (Bayer Crop Science), and Pyd (Syngenta) was assessed in the

556   WT and in edited strains on the basis of inhibition of germination. Assays with a range of fungicide

557   concentrations (0, 0.001, 0.003, 0.01, 0.03, 0.1, 0.3, 1, 3, 10 mg l^{-1}) were carried out at 20°C. After

558   incubation for 30 h in Greiner Bio-one polystyrene microtiter plates, the fraction of conidia containing

559   germ tubes with lengths exceeding half of the conidial diameters was determined for each

560   strain/fungicide pair, and an EC$_{50}$ value (effective fungicide concentration required to inhibit

561   germination by 50%) was calculated with the Graphpad Prism 5.01 software, using a normalized

562   response with variable slope fitted to log fungicide concentrations.

563 **Microscopy.** Confocal images were acquired using either a Leica SP5 (DM6000 CS), TCS acousto-optical
564 beam splitter confocal laser scanning microscope, equipped with a Leica HCX PL APO CS 63 × 1.20.
565 water-immersion objective or a Zeiss LSM880, AxioObserver SP7 confocal laser-scanning microscope,
566 equipped with a Zeiss C-Apochromat 40x/1.2 W AutoCorr M27 water-immersion objective.
567 Fluorescence signals of GFP (Leica: excitation/emission 488 nm/500-550 nm, Zeiss:
568 excitation/emission 488 nm/500-571 nm), were processed using Leica software LAS AF 3.1, Zeiss
569 software ZEN 2.3 or Fiji software.

570 **Protein analysis.** For in-gel detection of superoxide dismutase activity, *B. cinerea* conidia were
571 germinated in ME medium overnight, washed with extraction buffer (100 mM potassium phosphate
572 buffer (pH 7.8) 0.1 mM (EDTA) 1 % (w/v) polyvinyl-pyrrolidone (PVP) 0.5% (v/v) Triton X 100) the
573 mycelium ground with mortar and pestle in liquid nitrogen. Fifteen µg of cleared extract was separated
574 in an polyacrylamide gel and stained for SOD activity as described [69]. For detection of Cas9 Sod1-GFP
575 fusion proteins, *B. cinerea* protein extracts prepared as described above were separated in an SDS
576 polyacrylamide gel and subjected to an immunoblot on nitrocellulose, using monoclonal antibodies
577 against Cas9 (Clontech, Palo Alto, CA, USA) or GFP (Sigma), followed by chemiluminescent detection.

578 **Statistics and reproducibility.** Statistical analyses were carried out with the GraphPad Prism software.
579 The detailed analysis method is depicted in the individual figure legends. All experiments were carried
580 out at least three times. For growth and infection assays, three technical replicates per sample were
581 performed. Box limits of box plots represent 25th percentile and 75th percentile, horizontal line
582 represents median. Whiskers display minimum to maximum values. Bar charts represent mean values
583 with standard deviations.

584

585 **Acknowledgements**

References

592

593 1. Elad, Y, Pertot, I, Prado AMC & Stewart, A. Plant hosts of *Botrytis* spp. In: Elad Y, Vivier M, Fillinger
594   S (ed.), *Botrytis*, the good, the bad and the ugly. 413–486 (2016).

595 2. Dean, R. et al. The Top 10 fungal pathogens in molecular plant pathology. Mol. Plant Pathol. 13,
596   414–430 (2012).

597 3. Hahn, M. The rising threat of fungicide resistance in plant pathogenic fungi: *Botrytis* as a case
598   study. J. Chem. Biol. 7, 133–141 (2014).

599 4. van Kan, J. A. L. Licensed to kill: the lifestyle of a necrotrophic plant pathogen. Trends Plant Sc.
600   11, 247–253 (2006).

601 5. Müller, N. et al. Investigations on VELVET regulatory mutants confirm the role of host tissue
602   acidification and secretion of proteins in the pathogenesis of *Botrytis cinerea*. New Phytol. 219,
603   1062–1074 (2018).

604 6. Govrin, E. M. & Levine, A. The hypersensitive response facilitates plant infection by the
605   necrotrophic pathogen *Botrytis cinerea*. Current Biol. 10, 751–757 (2000).

606 7. Veloso, J. & van Kan, J. A. L. Many shades of grey in *Botrytis*-host plant interactions. Trends Plant
607   Sc. 23, 613–622 (2018).

608 8. Weiberg, A. et al. Fungal small RNAs suppress plant immunity by hijacking host RNA interference
609   pathways. Science 342, 118–123 (2013).

610 9. Cai, Q., He, B., Kogel, K.-H. & Jin, H. Cross-kingdom RNA trafficking and environmental RNAi-
611   nature's blueprint for modern crop protection strategies. Curr. Opin. Microbiol. 46, 58–64
612   (2018).

613 10. van Kan, J. A. L. et al. A gapless genome sequence of the fungus *Botrytis cinerea*. Mol. Plant
614   Pathol. 18, 75–89 (2017).

615 11. Hamada, W., Reignault, P., Bompeix, G. & Boccara, M. Transformation of *Botrytis cinerea* with
616   the hygromycin B resistance gene, hph. Curr. Genet. 26, 251–255 (1994).

617 12. Giesbert, S. et al. Identification of pathogenesis-associated genes by T-DNA-mediated insertional
618   mutagenesis in *Botrytis cinerea*: a type 2A phosphoprotein phosphatase and an SPT3
619   transcription factor have significant impact on virulence. Mol. Plant-Microbe Interact. 25, 481–
620   495 (2012).

621 13. Espino, J., González, M., González, C. & Brito, N. Efficiency of different strategies for gene
622   silencing in *Botrytis cinerea*. Appl. Microbiol. Biotechnol. 98, 9413–9424 (2014).

623 14. Schumacher, J. Tools for Botrytis cinerea: New expression vectors make the gray mold fungus
624   more accessible to cell biology approaches. Fungal Genet. Biol. 49, 483–497 (2012).

625 15. Hartmann, T. et al. Validation of a self-excising marker in the human pathogen *Aspergillus
626   fumigatus* by employing the beta-rec/six site-specific recombination system. Appl. Environ.
627   Microbiol. 76, 6313–6317 (2010).

628 16. Wright, A. V., Nuñez, J. K. & Doudna, J. A. Biology and applications of CRISPR systems: harnessing
629   nature's toolbox for genome engineering. Cell 164, 29–44 (2016).

630 17. Le Cong et al. Multiplex genome engineering using CRISPR/Cas systems. Science 339, 819–823
631   (2013).

632   18.   Mali, P. et al. RNA-guided human genome engineering via Cas9. Science 339, 823–826 (2013).

633   19.   Jinek, M. et al. A programmable dual-RNA-guided DNA endonuclease in adaptive bacterial
634   immunity. Science 337, 816–821 (2012).

635   20.   Sternberg, S. H., Redding, S., Jinek, M., Greene, E. C. & Doudna, J. A. DNA interrogation by the
636   CRISPR RNA-guided endonuclease Cas9. Nature 507, 62–67 (2014).

637   21.   Schuster, M. & Kahmann, R. CRISPR-Cas9 genome editing approaches in filamentous fungi and
638   oomycetes. Fungal Genet. Biol. 130, 43–53 (2019).

639   22.   Al Abdallah, Q., Ge, W. & Fortwendel, J. R. A simple and universal system for gene manipulation
640   in *Aspergillus fumigatus*: in vitro-assembled Cas9-guide RNA ribonucleoproteins coupled with
641   micro¬homology repair templates. mSphere 2: e00446-17. (2017).

642   23.   Foster, A. J. et al. CRISPR-Cas9 ribonucleoprotein-mediated co-editing and counterselection in
643   the rice blast fungus. Sci. Rep. 8, 14355 (2018).

644   24.   Wang, Q., Cobine, P. A. & Coleman, J. J. Efficient genome editing in *Fusarium oxysporum* based
645   on CRISPR/Cas9 ribonucleoprotein complexes. Fungal Genet. Biol. 117, 21–29 (2018).

646   25.   Leroch, M. et al. Living colors in the gray mold pathogen *Botrytis cinerea*: codon-optimized genes
647   encoding green fluorescent protein and mCherry, which exhibit bright fluorescence. Appl.
648   Environ. Microbiol. 77, 2887–2897 (2011).

649   26.   Barreau, C., Iskandar, M., Turcq, B. & Javerzat, J. P. Use of a linear plasmid containing telomeres
650   as an efficient vector for direct cloning in the filamentous fungus *Podospora anserina*. Fungal
651   Genet. Biol. 25, 22–30 (1998).

652   27.   Liu, W., Leroux, P. & Fillinger, S. The HOG1-like MAP kinase Sak1 of *Botrytis cinerea* is negatively
653   regulated by the upstream histidine kinase Bos1 and is not involved in dicarboximide- and
654   phenylpyrrole-resistance. Fungal Genet. Biol. 45, 1062–1074 (2008).

655   28.   Viaud, M. et al. A class III histidine kinase acts as a novel virulence factor in *Botrytis cinerea*. Mol.
656   Plant-Microbe Interact. 19, 1042–1050 (2006).

657   29.   Fillinger, S., Ajouz, S., Nicot, P. C., Leroux, P. & Bardin, M. Functional and structural comparison
658   of pyrrolnitrin- and iprodione-induced modifications in the class III histidine-kinase Bos1 of
659   *Botrytis cinerea*. PloS One 7, e42520 (2012).

660   30.   Cohrs, K. C., Burbank, J. & Schumacher, J. A new transformant selection system for the gray mold
661   fungus *Botrytis cinerea* based on the expression of fenhexamid-insensitive ERG27 variants.
662   Fungal Genet. Biol. 100, 42–51 (2017).

663   31.   Nødvig, C. S. et al. Efficient oligo nucleotide mediated CRISPR-Cas9 gene editing in Aspergilli.
664   Fungal Genet. Biol. 115, 78–89 (2018).

665   32.   Pohl, C., Kiel, J. A. K. W., Driessen, A. J. M., Bovenberg, R. A. L. & Nygård, Y. CRISPR/Cas9 based
666   genome editing of *Penicillium chrysogenum*. ACS Synth. Biol. 5, 754–764 (2016).

667   33.   Zhang, C., Meng, X., Wei, X. & Lu, L. Highly efficient CRISPR mutagenesis by microhomology-
668   mediated end joining in *Aspergillus fumigatus*. Fungal Genet. Biol. 86, 47–57 (2016).

669   34.   Dalmais, B. et al. The *Botrytis cinerea* phytotoxin botcinic acid requires two polyketide synthases
670   for production and has a redundant role in virulence with botrydial. Mol. Plant Pathol. 12, 564–
671   579 (2011).

672 35. Noda, J., Brito, N. & González, C. The *Botrytis cinerea* xylanase Xyn11A contributes to virulence
673   with its necrotizing activity, not with its catalytic activity. BMC Plant Biol. 10, 38 (2010).

674 36. Rolke, Y. et al. Functional analysis of H(2)O(2)-generating systems in *Botrytis cinerea*: the major
675   Cu-Zn-superoxide dismutase (BCSOD1) contributes to virulence on French bean, whereas a
676   glucose oxidase (BCGOD1) is dispensable. Mol. Plant Pathol. 5, 17–27 (2004).

677 37. Islinger, M., Li, K. W., Seitz, J., Völkl, A. & Lüers, G. H. Hitchhiking of Cu/Zn superoxide dismutase
678   to peroxisomes-evidence for a natural piggyback import mechanism in mammals. Traffic 10,
679   1711–1721 (2009).

680 38. Cuesta Arenas, Y. et al. Functional analysis and mode of action of phytotoxic Nep1-like proteins
681   of *Botrytis cinerea*. Physiol. Mol. Plant Pathol. 177, 376–386 (2010).

682 39. Wilson, R. A. & Talbot, N. J. Under pressure: investigating the biology of plant infection by
683   *Magnaporthe oryzae*. Nat. Rev. Microbiol. 7, 185–195 (2009).

684 40. Sierotzki, H. & Scalliet, G. A review of current knowledge of resistance aspects for the next-
685   generation succinate dehydrogenase inhibitor fungicides. Phytopathology 103, 880–887 (2013).

686 41. Veloukas, T., Markoglou, A. N. & Karaoglanidis, G. S. Differential effect of sdhB gene mutations
687   on the sensitivity to SDHI fungicides in *Botrytis cinerea*. Plant Dis. 97, 118–122 (2013).

688 42. Angelini, R. M., Masiello, M., Rotolo, C., Pollastro, S. & Faretra, F. Molecular characterisation and
689   detection of resistance to succinate dehydrogenase inhibitor fungicides in *Botryotinia fuckeliana*
690   (*Botrytis cinerea*). Pest Manag. Sci. 70, 1884–1893 (2014).

691 43. Muñoz, M., Faust, J. E. & Schnabel, G. Characterization of *Botrytis cinerea* from commercial cut
692   flower roses. Plant Dis. 103, 1577–1583 (2019).

693 44. Nødvig, C. S., Nielsen, J. B., Kogle, M. E. & Mortensen, U. H. A CRISPR-Cas9 system for genetic
694   engineering of filamentous fungi. PLoS One 10, e0133085 (2015).

695 45. Katayama, T. et al. Forced recycling of an AMA1-based genome-editing plasmid allows for
696   efficient multiple gene deletion/integration in the industrial filamentous fungus *Aspergillus*
697   *oryzae*. Appl. Environ. Microbiol. 85, pii: e01896-18 (2019).

698 46. Schuster, M., Schweizer, G., Reissmann, S. & Kahmann, R. Genome editing in *Ustilago maydis*
699   using the CRISPR-Cas system. Fungal Genet. Biol. 89, 3–9 (2016).

700 47. Wenderoth, M., Pinecker, C., Voß, B. & Fischer, R. Establishment of CRISPR/Cas9 in *Alternaria*
701   *alternata*. Fungal Genet. Biol. 101, 55–60 (2017).

702 48. Shi, T.-Q. et al. CRISPR/Cas9-based genome editing in the filamentous fungus *Fusarium fujikuroi*
703   and its application in strain engineering for gibberellic acid production. ACS Synth. Biol. 8, 445–
704   454 (2019).

705 49. Fillinger, S. et al. Genetic analysis of fenhexamid-resistant field isolates of the phytopathogenic
706   fungus *Botrytis cinerea*. Antimicrob. Agents Chemother. 52, 3933–3940 (2008).

707 50. Liu, R., Chen, L., Jiang, Y., Zhou, Z. & Zou, G. Efficient genome editing in filamentous fungus
708   *Trichoderma reesei* using the CRISPR/Cas9 system. Cell Discov. 1, 15007 (2015).

709 51. Gardiner, D. M. & Kazan, K. Selection is required for efficient Cas9-mediated genome editing in
710   *Fusarium graminearum*. Fungal Biol. 122, 131–137 (2018).

711 52. Zuris, J. A. et al. Cationic lipid-mediated delivery of proteins enables efficient protein-based
712   genome editing *in vitro* and in vivo. Nature Biotechnol. 33, 73–80 (2015).

713   53.   Allen, F. et al. Predicting the mutations generated by repair of Cas9-induced double-strand
714   breaks. Nature Biotechnol. 37, 64–72 (2019).

715   54.   Lemos, B. R. et al. CRISPR/Cas9 cleavages in budding yeast reveal templated insertions and
716   strand-specific insertion/deletion profiles. Proc. Natl. Acad. Sci. USA 115, E2040-E2047 (2018).

717   55.   Wernars, K. et al. Cotransformation of *Aspergillus nidulans*: a tool for replacing fungal genes.
718   Mol. Gen. Genet. 209, 71–77 (1987).

719   56.   Austin, B. & Tyler, B. M. Strategies for high-efficiency cotransformation of *Neurospora crassa*.
720   Exp. Mycol. 14, 9–17 (1990).

721   57.   Scalliet, G. Mutagenesis and functional studies with succinate dehydrogenase inhibitors in the
722   wheat pathogen *Mycosphaerella graminicola*. PLoS One 7(4), e35429 (2012).

723   58.   Veloukas, T., Kalogeropoulou, P., Markoglou, A. N. & Karaoglanidis, G. S. Fitness and competitive
724   ability of *Botrytis cinerea* field isolates with dual resistance to SDHI and QoI fungicides,
725   associated with several sdhB and the cytb G143A mutations. Phytopathology 104, 347–356
726   (2014).

727   59.   Lalève, A. et al. Site-directed mutagenesis of the P225, N230 and H272 residues of succinate
728   dehydrogenase subunit B from *Botrytis cinerea* highlights different roles in enzyme activity and
729   inhibitor binding. Environ. Microbiol. 16, 2253–2266 (2013).

730   60.   Lalève, A., Fillinger, S. & Walker, A.-S. Fitness measurement reveals contrasting costs in
731   homologous recombinant mutants of *Botrytis cinerea* resistant to succinate dehydrogenase
732   inhibitors. Fungal Genet. Biol. 67, 24–36 (2014).

733   61.   Mosbach, A. et al. Anilinopyrimidine resistance in *Botrytis cinerea* is linked to mitochondrial
734   function. Front. Microbiol. 8, 2361 (2017).

735   62.   Amiri, A., Heath, S. M. & Peres, N. A. Resistance to fluopyram, fluxapyroxad, and penthiopyrad
736   in *Botrytis cinerea* from strawberry. Plant Dis. 98, 532–539 (2014).

737   63.   Brent, K. J., Hollomon, D.W. Fungicide resistance: the assessment of risk (FRAC Monograph No.
738   2, Brussels, 1998). ISBN: 90-72398-07-6.

739   64.   Abdullah, T., Faiza, M., Pant, P., Rayyan Akhtar, M. & Pant, P. An analysis of single nucleotide
740   substitution in genetic codons - probabilities and outcomes. Bioinformation 12, 98–104 (2016).

741   65.   Anders, C. & Jinek, M. *In vitro* enzymology of Cas9. Meth. Enzymol. 546, 1–20 (2014).

742   66.   Leroch, M. et al. Gray mold populations in German strawberry fields are resistant to multiple
743   fungicides and dominated by a novel clade closely related to *Botrytis cinerea*. Appl. Environ.
744   Microbiol. 79, 159–167 (2013).

745   67.   Talbot, N. J., Ebbole, D. J. & Hamer, J. E. Identification and characterization of MPG1, a gene
746   involved in pathogenicity from the rice blast fungus *Magnaporthe grisea*. Plant Cell 5, 1575–
747   1590 (1993).

748   68.   Stammler, G. & Speakman, J. Microtiter method to test the sensitivity of *Botrytis cinerea* to
749   boscalid. J. Phytopathol. 154, 508–510 (2006).

750   69.   Lee, D.H. & Lee, C.B. Chilling stress-induced changes of antioxidant enzymes in the leaves of
751   cucumber: in gel enzyme activity assays. Plant Sci. 159, 75–85 (2000).
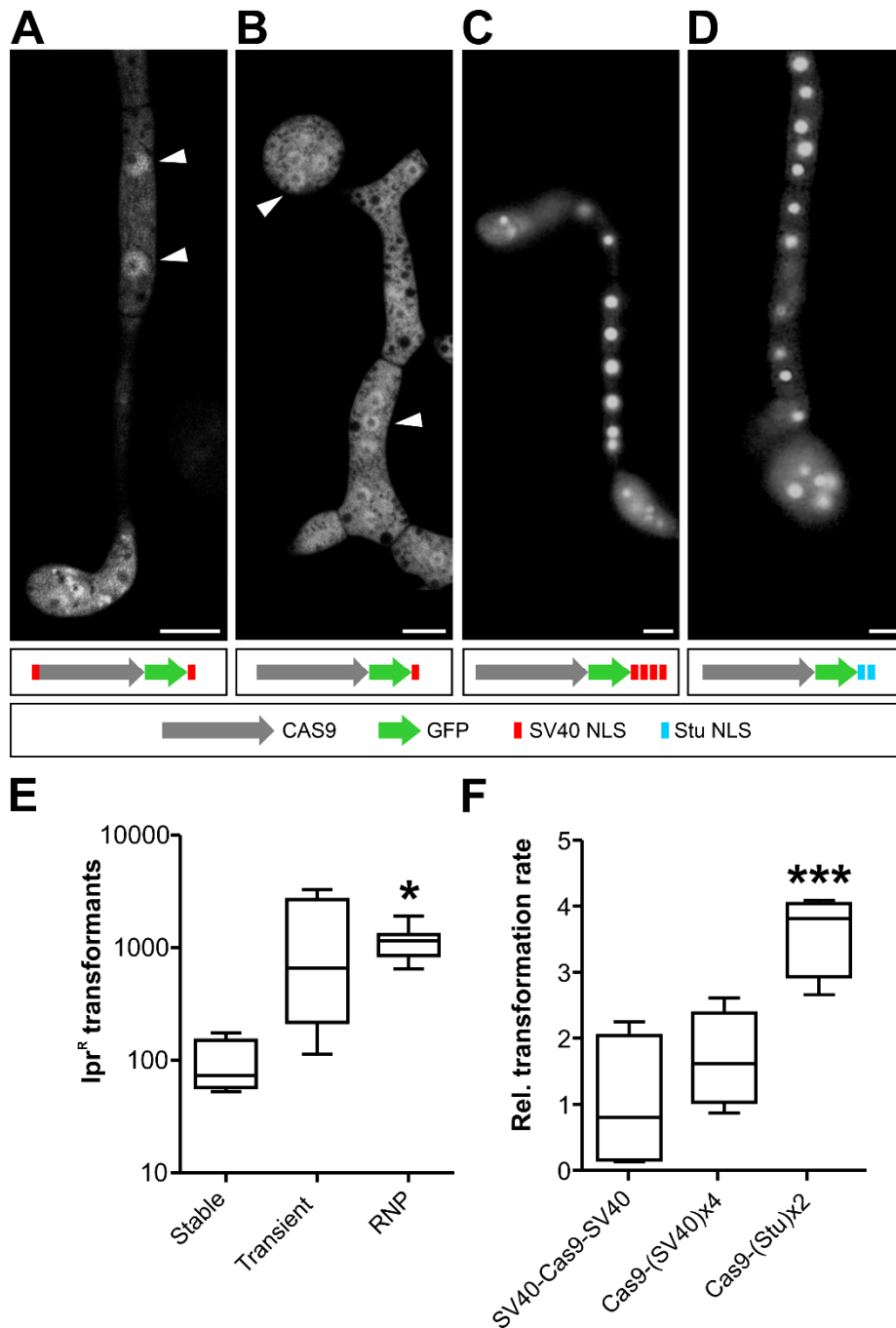
Fig. 1. Optimization of Cas9 nuclear targeting and delivery into *B. cinerea* protoplasts.

(A-D) Subcellular localization of genetically delivered Cas9-GFP constructs fused to different NLS. Fluorescence microscopy images of 18 h old germlings on glass slides. Arrowheads depict nuclei. Only in c and d, fluorescence is concentrated in the nuclei. Scale bars: 5 µm. (E) Transformation rates (NHEJ-mediated, Ipr^R *Bos1* k.o. transformants) obtained in *B. cinerea* with different Cas9 delivery strategies. Cas9 was expressed from a chromosomally integrated gene (Cas9-SV40^{x4}-NLS; stable), transiently from a gene on a telomere vector (Cas9-GFP-SV40^{x4}-NLS; transient) or added as a protein (Cas9-Stu^{x2}-NLS; RNP) together with Bos1-T2 sgRNA to *B. cinerea* protoplasts. The *p* values by one-way ANOVA followed by Tuckey's multiple comparisons post hoc test are indicated. *$p \leq 0.05$; stable (n=4), transient (n=4), RNP (n=11). (F) Comparison of different NLS arrangements on genome editing efficiency of Cas9-sgRNA RNPs targeting *Bos1*. Values are relative to transformation rate with SV40-Cas9-SV40. In (E) and (F), no Ipr^R colonies were obtained without Cas9. The *p* values by one-way ANOVA followed by Dunnett's multiple comparisons post hoc test are indicated. ***p value ≤ 0.001; n=4.
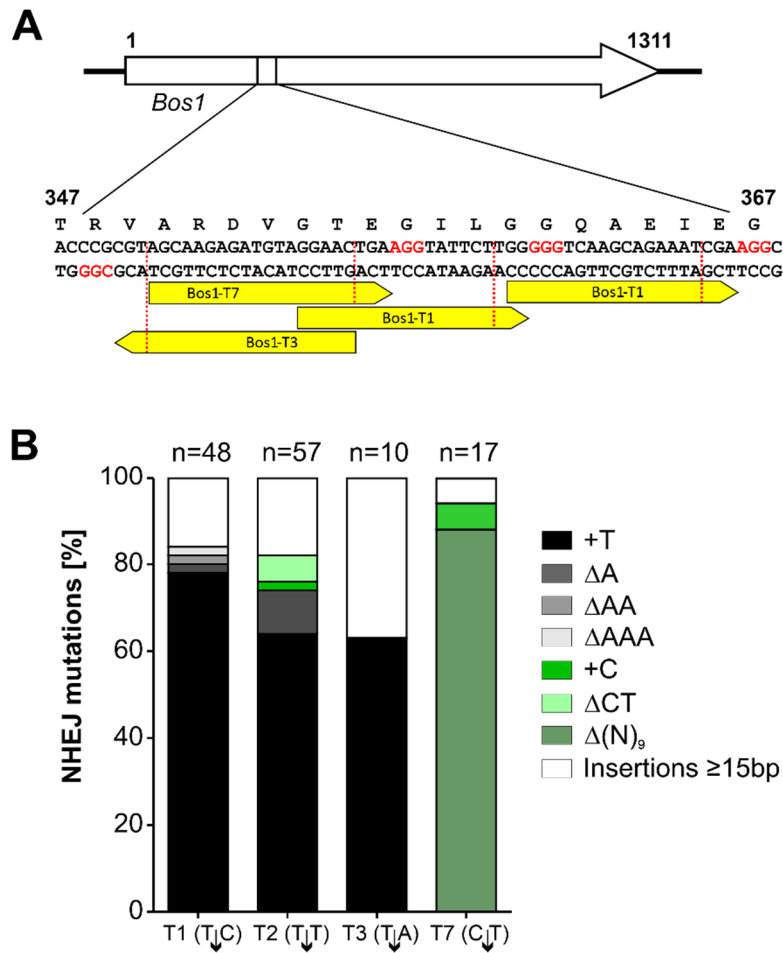
Fig 2. NHEJ-mediated mutations induced in *Bos1* by RNP mediated genome editing.

(A) Positions of the sgRNAs targeting *Bos1*. (B) Distribution of mutations detected in iprodione resistant transformants. Note that sgRNAs introducing T↓N cleavage sites resulted in a majority of '+T' insertions.

28
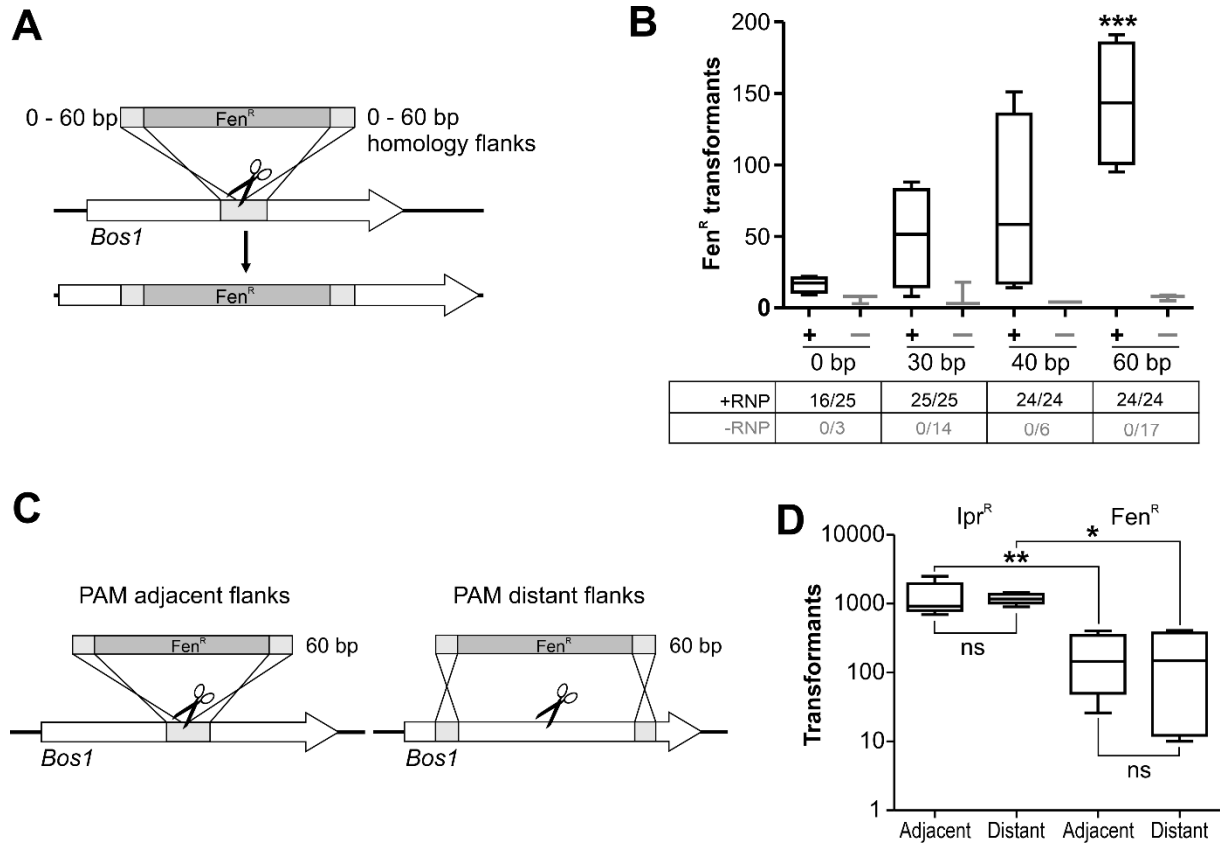
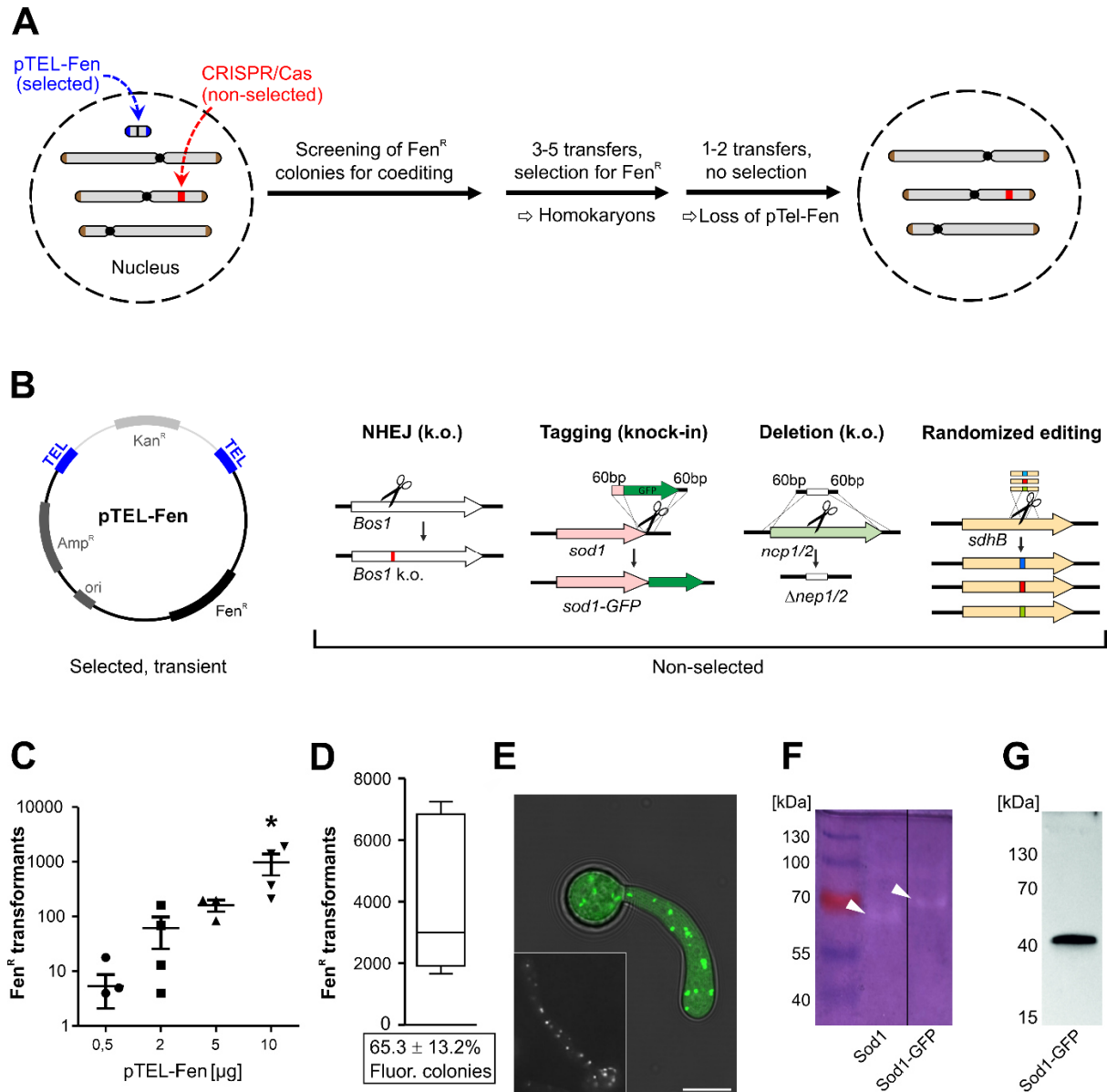**Fig. 3. Efficiency of CRISPR/Cas editing of *Bos1* using repair templates with short homology flanks**.
(A) Experimental scheme. (B) Results of transformations with RNP (black lines) and without RNP (gray lines) for RT with flank sizes of 0 to 60 bp. (+RNP: n=4; RNP: n=3). The numbers below show fractions of Fen[R] transformants being Ipr[R], indicating targeting efficiencies. The p values by one-way ANOVA followed by Dunnetts's multiple comparisons (control: 0 bp) post hoc test are indicated. ***p ≤ 0.001. (C) Scheme of *Bos1* targeting with different placement of 60 bp homology flanks of RT, resulting in insertion (left) or 2 kb deletion (right). (E) Results of transformations with RNP and two types of RT as shown in (C). n=5 (Ipr[R]); n=4 (Fen[R]). The *p* values by one-way ANOVA followed by Tukey's multiple comparisons post hoc test are indicated. *p ≤ 0.05; ** p ≤ 0,01.

A

Selected, stable

B
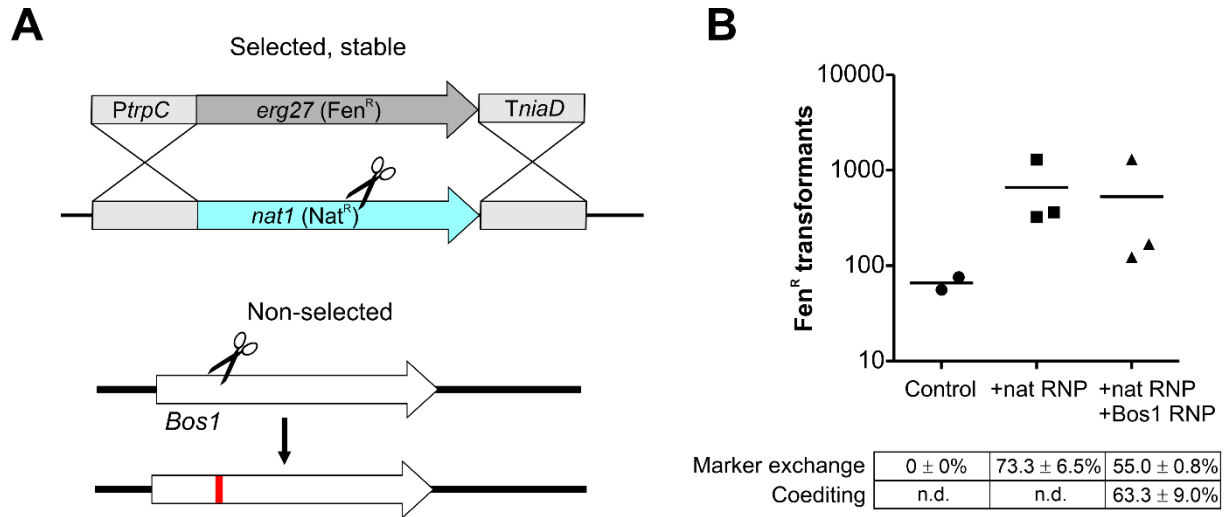
781
782
783
784 **Fig. 4. Application of marker exchange for non-selected CRISPR/Cas k.o. mutagenesis of *Bos1* via NHEJ.**
785 (A) Experimental scheme. (B) Results of transformation of *B. cinerea xyn11A*-Nat[R] with Cas9-RNP targeting *nat*
786 using Fen[R] RT, with or without Cas9-RNP targeting *Bos1*, as shown in (B). Control: Fen[R] RT transformed without
787 Cas9-RNP.

	Control	+nat RNP	+nat RNP +Bos1 RNP
Marker exchange	0 ± 0%	73.3 ± 6.5%	55.0 ± 0.8%
Coediting	n.d.	n.d.	63.3 ± 9.0%

Fig. 5. Telomere vector (pTEL)-mediated coediting for introduction of marker-free CRISPR/Cas edits into *B. cinerea*.

(A) Experimental setup. (B) Applications of non-selected editing performed in this study. pTEL-Fen can be propagated in *E. coli* with selection for ampicillin (Amp^R) and kanamycin (Kan^R). After transformation into *B. cinerea* it is linearized to a minichromosome with telomeric ends. (C) Transformation results for pTEL-mediated *Bos1* k.o. via NHEJ, depending on the amounts of pTEL-Fen added to the protoplasts. Individual data points are shown. The *p* values by one-way ANOVA followed by Dunnetts's multiple comparisons (control: 0.5 μg pTEL-Fen) post hoc test are indicated. *p $\leq$ 0.05. (D-G) Generation and characterization of a Sod1-GFP knock-in strain. (D) Transformation efficiency and frequency of fluorescent transformants (below; n=3). (E) Cytoplasmic and putative peroxisomal localization of Sod1-GFP fluorescence, as indicated by similar fluorescence pattern of a mutant expressing GFP fused to a SKL peroxisomal targeting motif [14]. (F) Native gel electrophoresis of *B. cinerea* protein extracts stained for superoxide dismutase activity. Lanes showing WT (expressing Sod1) and mutant (expressing Sod1-GFP, arrowheads). (G) Immunoblot detection of Sod1-GFP with GFP antibodies.
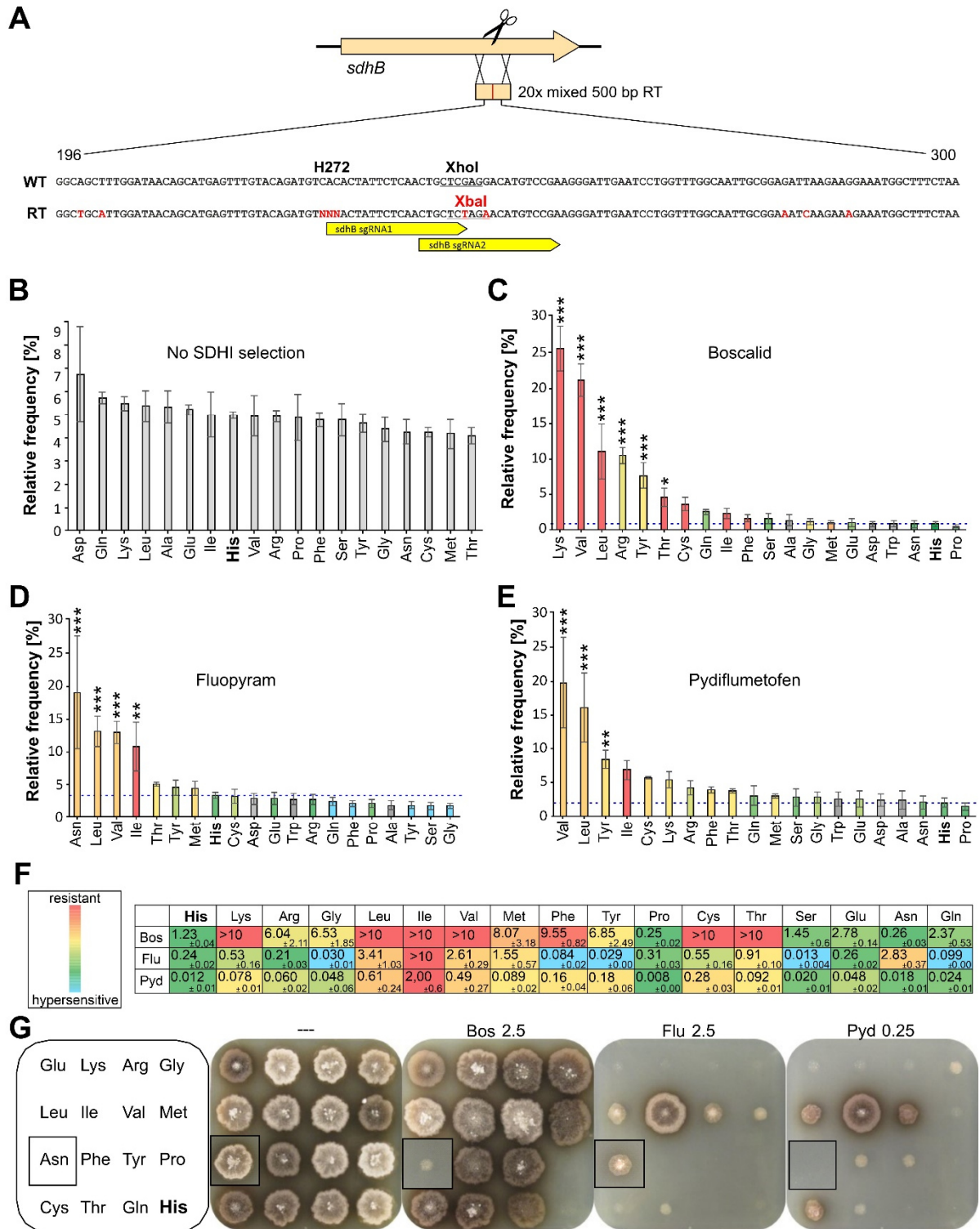
A **B**
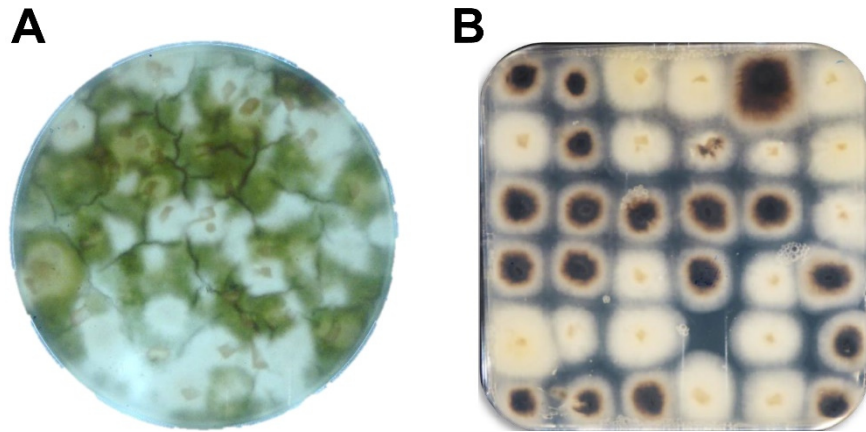
Fig. 6. Efficient pTEL-mediated coediting via NHEJ in *Magnaporthe oryzae*.

Protoplasts were cotransformed with pTEL-Fen and Cas9-ALB1-sgRNA RNP. (A) Primary selection plate containing fenhexamid. (B) Isolated transformants (transformation C, cf. S1 Table). Note white-colored mycelia of edited transformants.

810
811
812 **Fig. 7. Effects of *B. cinerea sdhB* codon 272 amino acid randomization by multiple editing.**
813 (A) Schematic strategy, showing sequences of WT and repair template (RT) surrounding codon 272. Changed
814 bases and the new restriction site in the RT are marked in red. NNN: Each of 20 codons in the RT mixture. (B-E)
815 Frequency distribution of encoded amino acids in codon 272 of edited *B. cinerea* transformants, determined by
816 deep sequencing of conidia obtained from primary Fen[R] transformants without SDHI fungicide selection (B), or
817 from cultures of transformed conidia incubated in YBA medium containing 0.25 mg l^{-1} Bos (C), 0.5 mg l^{-1} Flu (D),
818 or 0.15 mg l^{-1} Pyd. (E) Fungicide sensitivity levels conferred by each amino acid, as determined for the
819 corresponding mutant are indicated by colors (in (C-F)), except for the bars of amino acids for which no mutants
820 were obtained which are shaded in gray. The *p* values by one-way ANOVA followed by Dunnetts's multiple

33

821   comparisons (control: His) post hoc test are indicated. $*p \leq 0.05$, $**p \leq 0.01$, $***p \leq 0.001$ (n=3). (F) SDHI

822   sensitivity (EC_{50} values in mg l^{-1}) of individual mutants containing different amino acids in *sdhB* codon 272. (G)

823   Growth of individual codon 272 edited mutants on YBA agar containing different SDHI as indicated, after 5 days.

824   The inserts show colonies of an Asn mutant which were integrated into the pictures of plates with the other

825   mutants.

Supplementary Figures and Tables
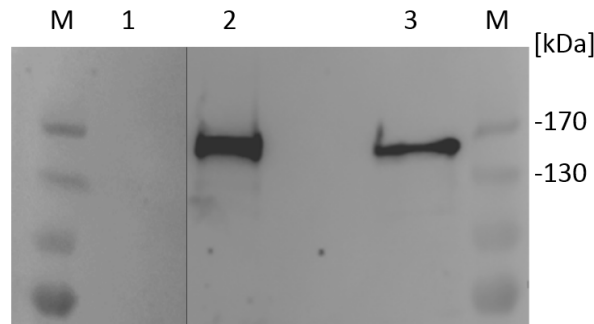
S1 Fig. Detection of Cas9 expression in *B. cinerea*.
Total *B. cinereal* protein extracts (15 µg per lane) were loaded, separated by polyacrylamide gel electrophoresis, and Cas9 detected with a monoclonal Cas9 antibody. M: Marker; 1: B05.10 (WT); 2: B05.10-Cas9-SV40[x4]; 3 B05.10 (pTEL-Cas9-Stu[x2]).
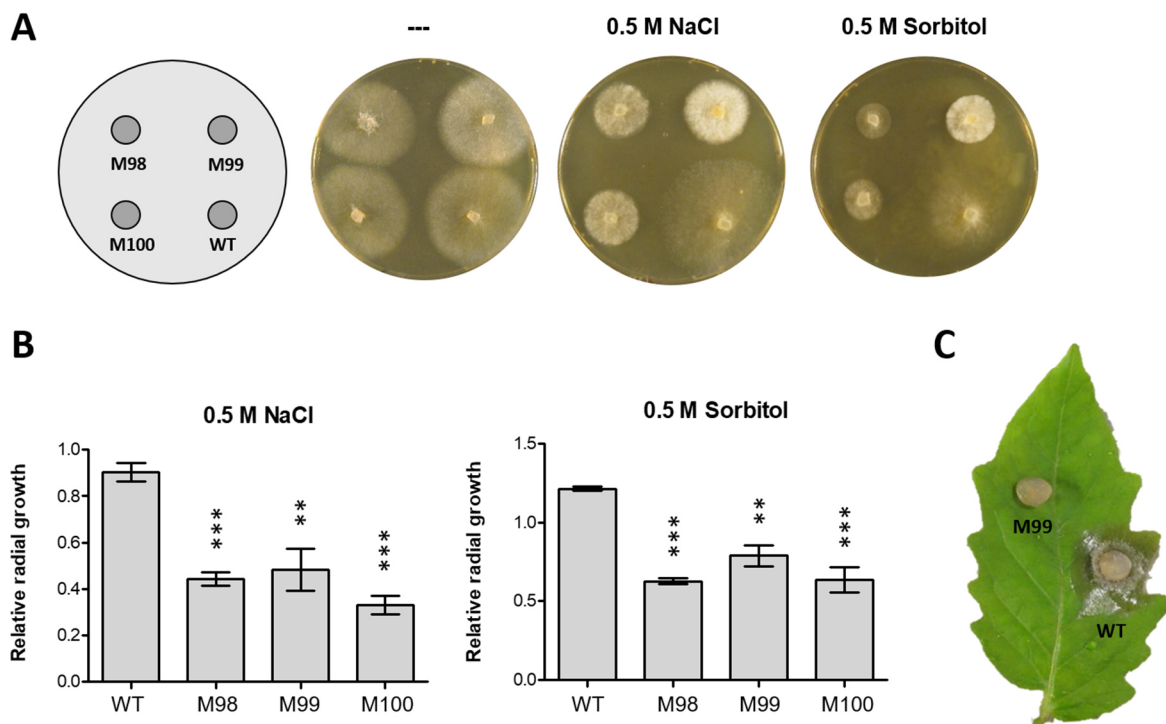

**S2 Fig. Sensitivity to osmotic and salt stress and virulence of *B. cinerea* WT and CRISPR/Cas-induced *Bos1* mutants.**
(A) Pictures of three Ipr[R] *Bos1* mutants (M98, M99, M100, all having the same '+T' insertion) and WT growth for 48 h on ME medium without (---) and with 0.5 M NaCl or sorbitol. (B) Effects of salt and osmotic stress treatments on radial growth, compared to growth on pure ME medium (n=3). The p values by one-way ANOVA followed by Dunnett's multiple comparisons (control: WT) post hoc test are indicated. $**p \le 0.01$; $***p \le 0.001$. (C) Infection on tomato leaf by WT and mutant M99 (72 h).

35
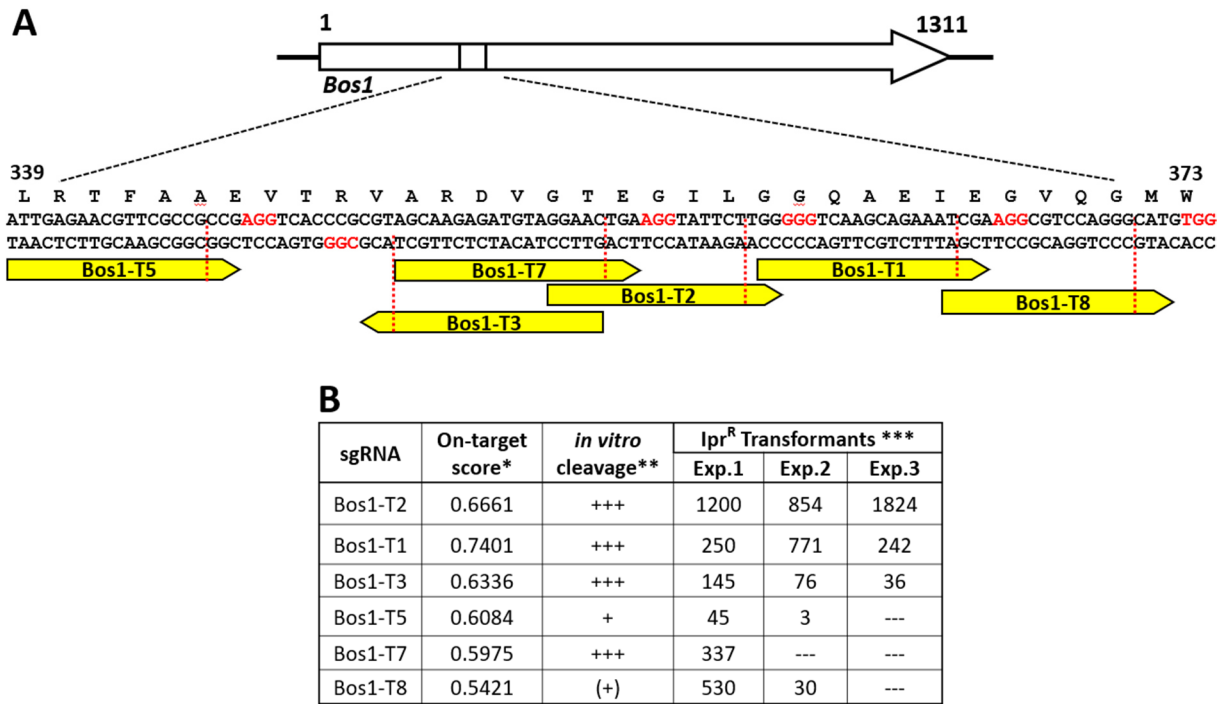
S3 Fig. *In vitro* and *in vivo* CRISPR/Cas performance of different sgRNAs targeting *Bos1*.
(A) Positions and expected cleavage sites (red dotted lines) of the sgRNAs (yellow) in *Bos1*. PAM sequences for each of the sgRNAs are indicated in red. (B) Summary of on-target scores, *in vitro* cleavage activities, and transformation efficiencies with different sgRNAs. *On-target efficiency calculated with the Broad Institute GPP sgRNA Designer. **Estimated from gel pictures. *** Number of Ipr[R] *B. cinerea* mutants per assay.

845

846

847

848

849

850

851
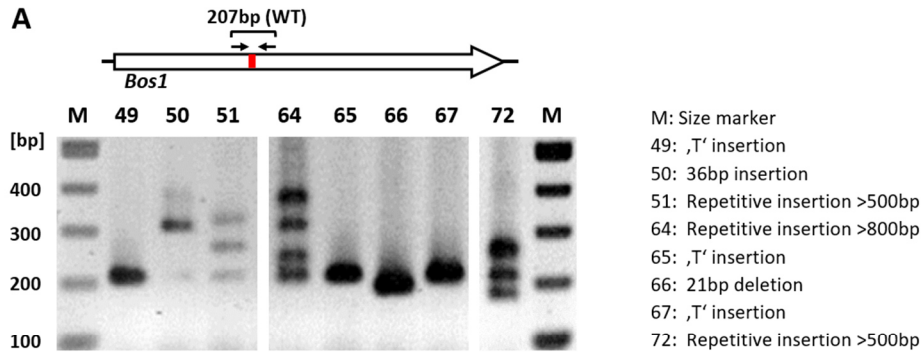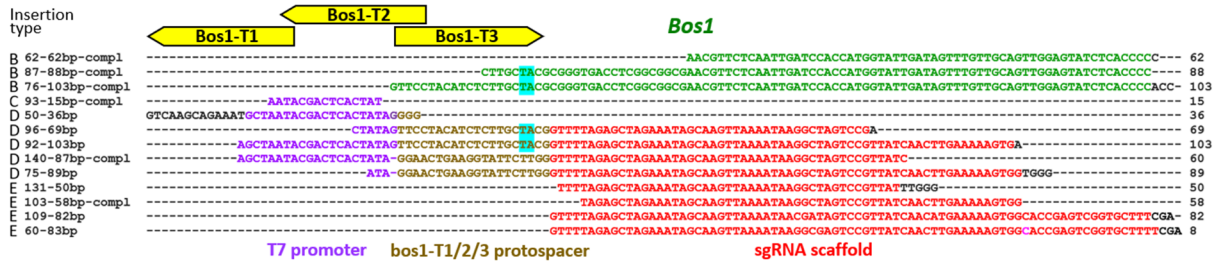
S4 Fig. Analysis of PCR fragments covering CRISPR/Cas-induced cleavage-repair sites in *Bos1*, from Ipr[R] transformants.

(A) Stained agarose gel with PCR fragments generated with primers TL_87 Bos1_check 200 Fw/ TL_87 Bos1_check 200 Rv, showing variations of fragment sizes due to different types of NHEJ-induced mutations in transformants obtained with Cas9/bos1-T1 RNP. (B) Origins and sequences of different NHEJ insertion types obtained with different Cas9/bos1 RNPs. Type A (not shown): 164 bp *B. cinerea* mitochondrial DNA, two joined fragments of 84 and 79 bp. Type B: *B. cinerea Bos1*-DNA. Type C: 15 bp fragment of the sgRNA scaffold encoding part of the T7 RNA polymerase promoter. Type D: sgRNA scaffold DNA containing part or all of the protospacer sequences of bos1-T1/-2/-3. Type E: sgRNA scaffold DNA lacking protospacer sequences.
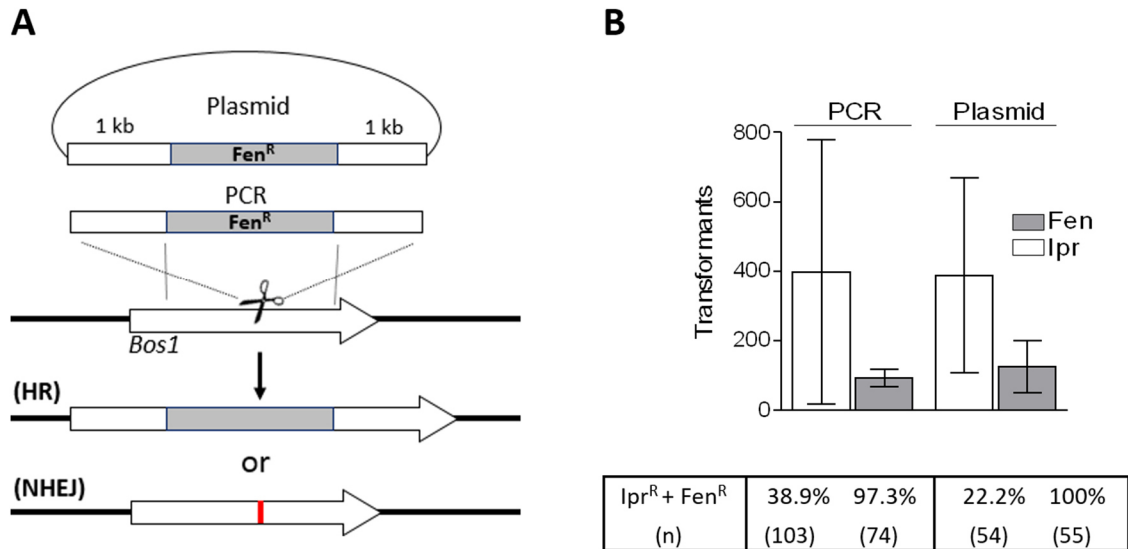
| Ipr^R + Fen^R	38.9%	97.3%	22.2%	100%
(n)	(103)	(74)	(54)	(55)

S5 Fig. Transformation of Cas9/*Bos1*-T2B-gRNA RNP and Fen^R RT with 1 kb *Bos1* homology flanks.

(A) Experimental scheme. *Bos1* inactivation leading to Ipr^R occurs either by targeted integration of the Fen^R RT via HR, or via NHEJ. (B) Transformation results: Primary selection was either for Ipr^R (white bars) or for Fen^R (grey bars) (n=3). Below the diagram, the fraction of transformants with resistance to both fungicides is shown. (n): Number of transformants tested. Statistical analyses were performed by analysis of variance (ANOVA, followed by Dunnett's multiple comparisons. No significant differences between transformation results with PCR fragments and circular plasmids, or between Ipr^R and Fen^R colony numbers were observed.
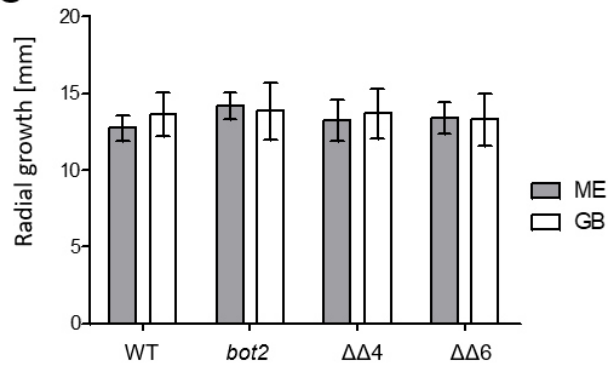
A

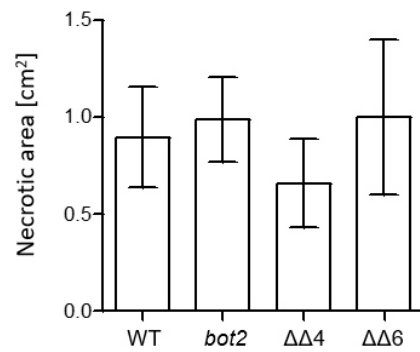| Assay	Target gene	sgRNA	Repair template	Transformants Fen^R	Transformants Cyp^R
A	*bot2*	1 μg	1 μg	8	3
	boa6	1 μg	1 μg		
B	*bot2*	2 μg	2 μg	39	14
	boa6	2 μg	2 μg		
C	*bot2*	2 μg	4 μg	46	16
	boa6	2 μg	4 μg		

B

C

D
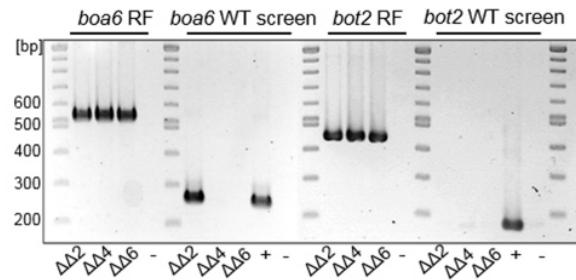
S6 Fig. CRISPR/Cas-HR-mediated single and double k.o. mutagenesis of *bot2* and *boa6*.
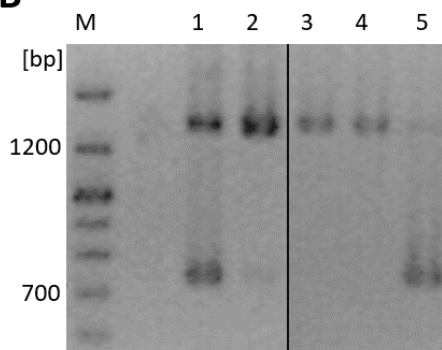
(A) Transformation results. (B) PCR-based verification of *bot2 boa6* double (ΔΔ) k.o. mutants. *boa6* RT right flank (RF) integration screen using primers TniaD_ol_Cyp_Fw/TL129 (537 bp); *boa6* WT screen using primers TL157/TL158 (263 bp), *bot2* RT RF integration screen using primers TL130/TL132 (444 bp), *bot2* WT screen using primers TL133/TL159 (180 bp). (C) Growth of WT and mutants after 72 h on agar plates with rich (ME) and minimal (GB: Gamborg GB5 with 25 mM glucose) medium (one way ANOVA; n=3). (D) Lesion formation after 72 h on tomato leaves (one way ANOVA; n=3). In (C) and (D), no significant differences in radial growth and infection between WT and mutants were observed.
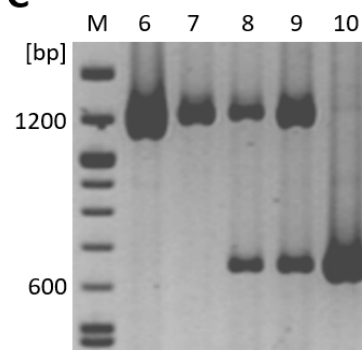
39

A

| pTEL-Fen	sgRNA (2 µg)	Δnep1 RT	Δnep2 RT	Total Fen^R transformants	Fraction of k.o. transformants (%)
10 µg	nep1-1	10 µg	---	1784	Δnep1: 7/30 (23.3)
10 µg	nep2-1	---	10 µg	3000	Δnep2: 5/30 (16.7)
10 µg	nep1-1 nep2-1	10 µg	10 µg	230	Δnep1: 9/70 (12.9) Δnep2: 7/70 (10.0) Δnep1 Δnep2: 0/70 (0)

B

C

S7 Fig. Use of pTEL-Fen for marker-free k.o. mutagenesis of *nep1* and *nep2*.

(A) Transformation result. (B) PCR-based verification of *nep1* deletion mutants, using primers TL143/TL144; size of WT fragment 1,353 bp, size of *nep1* k.o. fragment 733 bp. Lanes 1-5: Fen^R transformants. Transformant #5 represents a nearly pure *nep1* mutant. (C) PCR-based verification of *nep2* deletion mutants, using primers TL145/TL146; size of WT fragment 1,220 bp, size of *nep2* k.o. fragment 641 bp. Lane 6: *B. cinerea* WT; lanes 7-10: Fen^R transformants. Transformant #10 represents a purified *nep2* mutant. M: DNA marker.

A

MoALB1
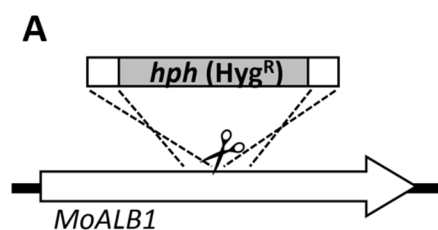
B

Transfo code	*M. oryzae* strain	Cas9-SV40^{x4}	sgRNA	Hyg-ALB1 RT	Hyg^R colonies	White colonies	Targeting efficiency
A	Guy11	6 µg	2 µg	6.6 µg	22	20	91%
B	Guy11 ku80	6 µg	2 µg	4 µg	18	18	72%
B	Guy11 ku80	6 µg	2 µg	4 µg	18	12	67%

S8 Fig. CRISPR/Cas efficiency with RNP in *M. oryzae*.

(A) Scheme of CRISPR/Cas targeting of *MoALB1*, using a repair template with a hygromycin resistance cassette and 50 bp homology flanks. (B) CRISPR/Cas components used and results of transformations with *M. oryzae* strain Guy11 and Guy11 ku80.

A

M. oryzae strain	Cas9-SV40[x4]/ sgRNA	Hyg-PIT RT	pTEL-Fen	Fen[R] colonies		Fen[R] Hyg[R] colonies/ k.o.s via HR
				Total	Tested	
Guy11 ku80	6 µg/ 2 µg	25 µg	6 µg	ca. 300	72	6/0
Guy11	6 µg/ 2 µg	25 µg	6 µg	ca. 670	72	23/5

B
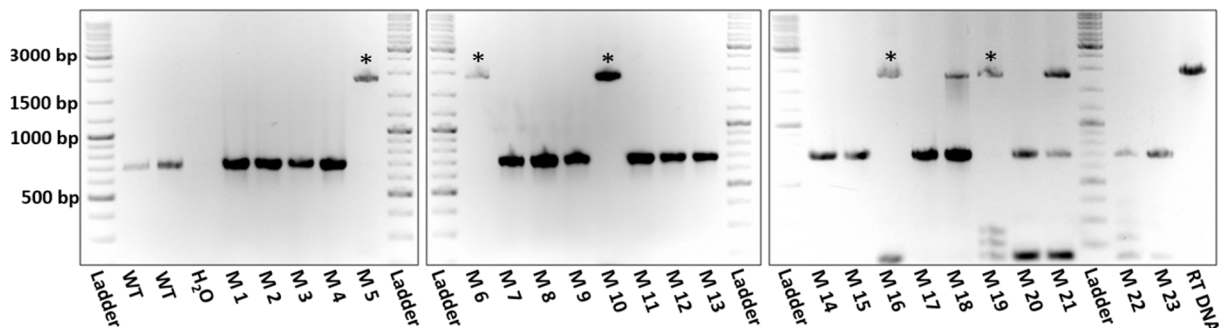
S9 Fig. pTEL-mediated k.o. of *MoPIT* via HR in *M. oryzae.*
(A) Results of transformations with strains Guy11 and Guy11ku80. (B) PCR-based identification of strain Guy11 *MoPIT* k.o. mutants generated by coediting, using primers MoPit FL F and MoPit FL R. HR was confirmed by sequencing PCR product amplified with primers SeqPit_F/ SeqPit_R.
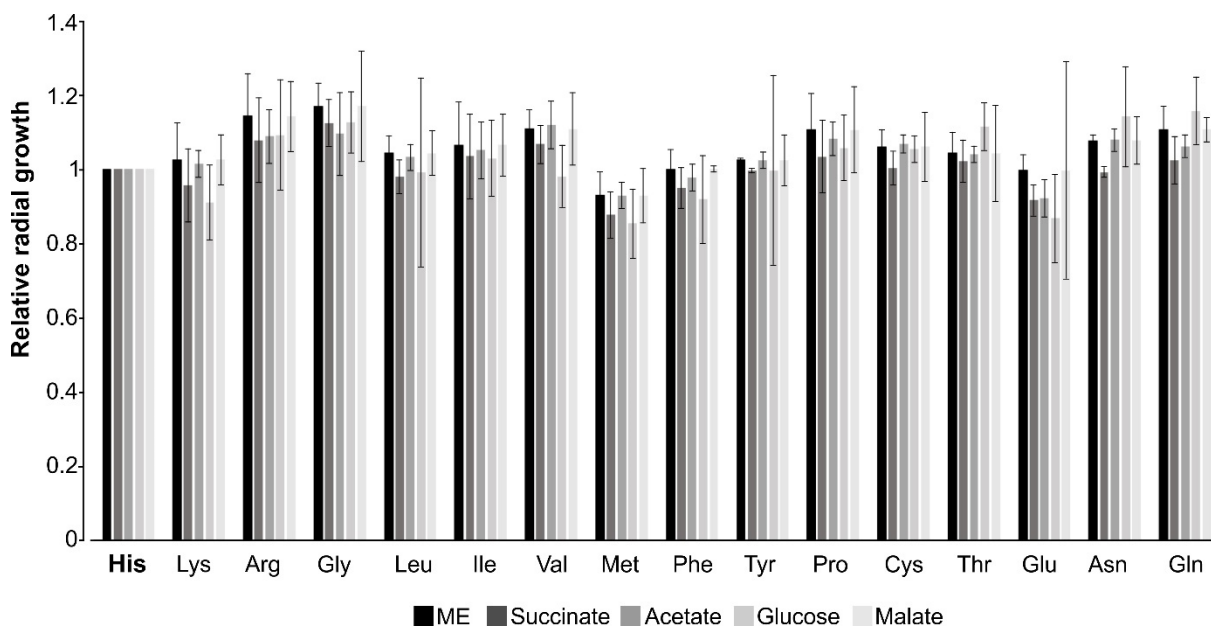
S10 Fig. Mycelium growth after 72 h of *B. cinerea sdhB* codon 272 exchange mutants on agar media containing ME or YSS with different carbon sources (50 mM each), relative to the WT strain (n=3).
Statistical analyses were performed by analysis of variance (ANOVA) followed by Dunnett's multiple comparisons (control: His). No significant differences between the growth rates of the WT strain (His) and any of the mutants were observed.

41

916 **S1 Table. pTEL-mediated coediting via NHEJ in *M. oryzae.***
917 CRISPR/Cas components used and results of (co-) transformations with strain Guy11 and Guy11 ku80.
918 Transformations with the same letter were done with the same batch of protoplasts.
919

Experi-ment	*M. oryzae* strain	Cas9-SV40x4/ sgRNA amounts	pTEL-Fen	Total	Tested	White Hyg[R] colonies (coediting rate)
B	Guy11	---	1 µg	18	---	---
B	Guy11	---	2 µg	200	---	---
C	Guy11	---	2 µg	555	---	---
C	Guy11	---	4 µg	3,800	---	---
D	Guy11	---	4 µg	4,000	---	---
D	Guy11 ku80	---	4 µg	3,000	---	---
E	Guy11 ku80	---	12 µg	1,500	---	---
E	Guy11 ku80	6 µg/ 2 µg	12 µg	300	72	5 (7%)
B	Guy11	6 µg/ 2 µg	6 µg	96	36	17 (47%)
C	Guy11	6 µg/ 2 µg	6 µg	280	35	17 (49%)
C	Guy11	6 µg/ 2 µg	3 µg	120	36	13 (36%)

920

921

922

923

924

925 **S2 Table. Results of cotransformation of *B. cinerea* with pTEL-Fen, sdhB272-sgRNA-RNP and 500 bp**
926 **sdhB-272 (x20) repair template.**
927

Transfor-mation[1]	sgRNA	Fen[R] colonies/ transformation	Sequenced transformants	Editing frequency	
				Counted[2]	Illumina seq.
A	sdhB272-1	820	---	9/72 (12.5%)	n.a.
A	sdhB272-2	1,100	---	12/96 (12.5%)	n.a.
B	sdhB272-1	2,680	---	10/41 (24%)	n.a.
C	sdhB272-2	2,200	---	11/26 (41%)	n.a.
D	sdhB272-2	4,820	6,100	n.a.	31.6
E	sdhB272-2	6,680	6,200	n.a.	21.4
F	sdhB272-1	7,080	10,400	n.a.	11.4

928 [1] $2x10^7$ protoplasts were transformed with 10µg pTEL-Fen, 6µg Cas9-2µg sdhB272-RNP, and 10µg *sdhB*-272(x20)
929 repair template. [2]To determine the fraction of edited transformants, DNA of individual transformants was
930 prepared, amplified with primers TL151_SdhB_OS_F/ TL152_SdhB_OS_R covering the edited region, and
931 digested with either XhoI (cut in WT *sdhB* DNA) or XbaI (cut in edited *sdhB* DNA). n.a.: Not analysed.

932 **S3 Table. Oligonucleotides used**

Name	5' to 3' sequence	Purpose
s	GATCTAGGCCTGCAGGATG	Generation of pFB2N from pFAC1
pFAC1-del2	CTAGCATCCTGCAGGCCTA	
FB108	TTATACAGCTGAGCAAATCGCCGGCGATCAGCATG	Truncation of pFB2N
FB109	CTGATCGCCGGCGATTTGCTCAGCTGTA	
bos1-checkF	GGGTGAGATACTCCAACTGCAA	Sequencing of *Bos1* mutants
bos1-checkR	CGCACTTGTGTGGTGAGGTTA	
TL29 pBS_ol_bos 3.REV	CGGGCCCCCCCTCGAGGTCGACGGTATCGATAAGCTTGATCTCTCCAGATGCCTCGACA	Generation of *Bos1* insertion construct with a Fen^R cassette
TL30 pBS_ol_*Bos1* 3.FOR	GATGTATCAGTGAGCCTAGGTGGGGGTCAA	
TL31 pBS_ol_*Bos1* 1.FOR	CTCTAGAACTAGTGGATCCCCCGGGCTGCAGGAATTCGATTCACAGTCAATAATCAAACCCTGC	
TL32 pBS_ol_*Bos1* 1.REV	CCAGCCAAGCCCAAAAAATGAGAATACCTTCAGTTCCTACATCTCTTGCTACG	
TL33 Fen_ol_*Bos1* 2.FOR	GTAGGAACTCAAGGTATTCTCATTTTTTGG	
TL34 Fen_ol_*Bos1* 2.REV	CGATTTCTGCTTGACCCCCACCTAGGCTCA	
TL37_Fen_fw	CATTTTTTGGGCTTGGCTGGAG	Fen^R cassette
TL38_Fen_rev	AGGCTCACTGATACATCTGGC	
TL65_*Bos1*_Fen30_fw	AGCAAGAGATGTAGGAACTGAAGGT	Synthesis of RTs targeting *Bos1* amplified from pBS_bos1_KO_Fen
TL66_*Bos1*_Fen30_rev	TGGACGCCTTCGATTTCTGCT	
TL67_*Bos1*_Fen40_fw	TCACCCGCGTAGCAAGAGAT	
TL68_*Bos1*_Fen40_rev	CCACATGCCCTGGACGC	
TL69_*Bos1*_Fen60_fw	GAGAACGTTCGCCGCCG	
TL70_*Bos1*_Fen60_rev	ACGTTCACTATCAATGTGTTCCACATG	
TL113 60bp Bos1 PD FW	GAACGAGAACTTGCGGCCTTGGTATCCAGAGTCCAAAGATTAGAAGCAAGGGCGATCACATGCTGGCCTTTTGCTCACATGCATG	PAM distant RT targeting *Bos1* amplified from pTEL-Fen
TL114 60bp Bos1 PD RV	TTGAATACTGTCCCTCAGATTGTACACCATCTGGTTGATCTTTCGCTTCAGCTCATCCATATCGCCGGAAAGGACCCGCAAATG	
TL116 Sod_GFP FW	GCTTGTGGTATGTTATTCCTTCTATGAAGATGCAGTTTCTGGACACATGACTAACATCATCACAGGTGTTATCGGTATTGCTGCAATGGTTTCCAAGGGTGAGGTAAGTA	RT synthesis for *sod1*-GFP fusion amplified from pNAH-OGG
TL134 Sod-GFP no R RV	GATTGCTTTTCTGTTAAAACTACCTAGACACAGCCGGCAAACTAAGCTAAATGATCCATACTAAGCGGCCGCTTTGTAAAGTTC	
TL 170 Nep1 KO F	CAGCATCAACAGCATCAGCTTCCATTCCATATTCATTACATTCCACATTACCACTTTCGTATCGCCGGAAAGGACCCGCAAATG	RT synthesis for marker-free *nep1* k.o.
TL 171 Nep1 KO R	ACGATCTCTGACAGGACAAACTTCCAGATTCTCCAGAACTCTATCTAGTAAGAAAGAACTTGCTGGCCTTTTGCTCACATGCATG	
TL 172 Nep2 KO F	CACACATCTATTAATCGCTCTCTCCTCTTAGTTACAAGGAAAATCCAGACAAACTTCATCTGCTGGCCTTTTGCTCACATGCATG	RT synthesis for marker-free *nep2* k.o.
TL 173 Nep2 KO R	GCAAAAGCCAATAGACTCCCAGAATATAGCCCCTTATATTCATACATAAAGACACAAAGTATCGCCGGAAAGGACCCGCAAATG	
TL143 Nep1 seq F	TCTGGTGCCGATTGAATACATCAAGTG	Check for *nep1* k.o.
TL144 Nep1 seq R	CGTTGGCTTATTCAATGCGGAGG	
TL145 Nep2 seq F	GAACTTTGAATAGTGGGCAGTTGGG	Check for *nep2* k.o.
TL146 Nep2 seq R	ACAAGGCGACCATGATTATTTCTGG	
TL118 boa6 RT FW	CTCCATTGAAAAAGCTGAGTTTTCGCAACCTCTTTGCACAGCCCTACAGATTGCTCTTGTTGCTGGCCTTTTGCTCACATGCATG	RT synthesis for *boa6* k.o. (Cyp^R marker)
TL 119 boa6 RT RV	GCAAAAACGCCTCTATCGTCAAGTGTCGACTTTGCTTTTTCGATAGCATCTTTGTTGCCGATCGCCGGAAAGGACCCGCAAATG	
TniaD_ol_CypR_FW	ACCATCCTTTTGGCGAAGAATAAGTAACTGAGAGGTGGTTTAGATATGG	Integration check *boa6* k.o.
TL 129 Boa6 KO R	CTTTTGCAGCTATGCTGACGGCCTCG	
TL157 Boa6 WT FW	GGGGTCACATTCTCTGCTGTAGTCGG	Check for WT nuclei in *boa6* k.o.
TL158 Boa6 WT RV	GTGACTGTCTTTGGAGCATTACTAGCCGC	
TL 120 Bot2 RT FW	AAGGACACCTGAAGGAAGATCCCGCCGCCGCAGCGGAGGAGGTGAAGCAGACCATTGCCATGCTGGCCTTTTGCTCACATGCATG	RT synthesis for *bot2* k.o. (Fen^R marker)
TL 121 Bot2 RT RV	CCTTGACTGGACACAGCTTTTAACCGATCCCAACATTGTTGGAAGACATATCGAATGGGAATCGCCGGAAAGGACCCGCAAATG	
TL 130 Fen check F	AACTGGGCGCCGAATGCTGGG	Integration check *bot2* k.o.
TL 132 Bot2 KO R	TCGTCAAGCCATGCCAGAGACTCGTGG	
TL 133 Bot2 KO F	CGACGATCGTACGTTGCTCTTAGTCATTGGACG	Check for WT nuclei in *bot2* k.o.
TL159 Bot2 WT RV	GACTCGGCAGTATACCGTGGTGCATTCC	
TL147 gRNA_rev	AAAAGCACCGACTCGGTGCCACTTTTTCAAGTTGATAACGGACTAGCCTTATTTTAACTTGCTATTTCTAGCTCTAAAAC	Constant oligonucleotide for sgRNA synthesis
gRNA Bos1-T1	AAGCTAATACGACTCACTATAGGGGGTCAAGCAGAAATCGAGTTTTAGAGCTAGAAATAGCAAG	sgRNA targeting *Bos1*
gRNA Bos1-T2	AAGCTAATACGACTCACTATAGGAACTGAAGGTATTCTTGGGTTTTAGAGCTAGAAATAGCAAG	sgRNA targeting *Bos1*
gRNA Bos1-T3	AAGCTAATACGACTCACTATAGTTCCTACATCTCTTGCTACGGTTTTAGAGCTAGAAATAGCAAG	sgRNA targeting *Bos1*
TL25 Bos1-T5 gRNA	AAGCTAATACGACTCACTATAGATTGAGAACGTTCGCCGCCGGTTTTAGAGCTAGAAATAGCAAG	sgRNA targeting *Bos1*

TL26 Bos1-T7 gRNA	AAGCTAATACGACTCACTATAGCAAGAGATGTAGGAACTGAGTTTTAGAGCTAGAAATAGCAAG	sgRNA targeting *Bos1*
TL27 Bos1-T8 gRNA	AAGCTAATACGACTCACTATAGTCGAAGGCGTCCAGGGCATGGTTTTAGAGCTAGAAATAGCAAG	sgRNA targeting *Bos1*
TL 107 Sod gRNA 1	AAGCTAATACGACTCACTATAGCACATGACTAATATCTTCACGTTTTAGAGCTAGAAATAGCAAG	sgRNA targeting *sod1*
TL125 Nat gRNA1	AAGCTAATACGACTCACTATAGCTGACCGTCGAGGACATCGGTTTTAGAGCTAGAAATAGCAAG	sgRNA targeting *nat*
TL 166 Bcnep1 gRNA	AAGCTAATACGACTCACTATAGCGCTTGGGTCAACAACCCCGGTTTTAGAGCTAGAAATAGCAAG	sgRNA targeting *nep1*
TL 168 Bcnep2 gRNA	AAGCTAATACGACTCACTATAGTATGTTCGAGGAGGACAAAGGTTTTAGAGCTAGAAATAGCAAG	sgRNA targeting *nep2*
TL141_ SdhB-1_gRNA	AAGCTAATACGACTCACTATA*g*ACACTATTCTCAACTGCTCGGTTTTAGAGCTAGAAATAGCAAG	sgRNA targeting *sdhB*
TL142_ SdhB-2_gRNA	AAGCTAATACGACTCACTATAGCTGCTCGAGGACATGTCCGAGTTTTAGAGCTAGAAATAGCAAG	sgRNA targeting *sdhB*
TL148_ SdhB_RT_F	AGGAAAAGAATACTTGCAATCTAAGGAGGATCGTAAG	Amplification of 500bp *sdhB* codon 272 mixed RT
TL149_ SdhB_RT_R	ACAATGGCTTGGCTTGGAGGACAATG	
TL151_SdhB_OS_F	CCATATCTTCAACACACCGACCCAGCACC	Check for *sdhB* editing
TL152_SdhB_OS_R	GCCCCCGAATATAATCCAACCCTTCTGAGAGG	
sdhb_F1	CATTAAGCCATATCTTCAACACACC	Primary and nested PCR for Illumina sequencing of *sdhB*
sdhb_R1	TATGGCTCTTCTTTCACTTGCATTC	
sdhb_F2	AGAGTTACAGATGGCTTGCAGATTC	
sdhb_R2	ACTTAGCAATAACCGCCCAAAAC	
MoPit FL F	ATGAGGTTTTCTACGGCCTTTCTC	Verification of *MoPIT* k.o.
MoPit FL R	CAAGTCACCCCATGGAGTGG	
MH-AlbF	GCCGCCACAAGCTCCCTCACCAAGGCCACGGCCATCCCGGTCCAATGCGTTTTATTCTTGTTGACATG	Amplification of *hph* with 50bp homologous flanks of *MoALB1*
MH-Alb R	GCAGAGCCTCTTGCATGAAACCTTGAAGCTGCTTGGCCTGCTCACTGGCCGTCGTTTTAC	
MH-Pit F	ATGAGGTTTTCTACGGCCTTTCTCGCCCTGCTCTCGGTCGGATGACAATGCGTTTTATTCTTGTTGACATGG	Amplification of *hph* with 50bp homologous flanks of *MoPIT*
MH-Pit R	CTACAAGTCACCCCATGGAGTGGCAATGCTATTCCTCTCACTCACTGGCCGTCGTTTTAC	
SeqPit_F	GCACTCCTGGTATCTACTGCC	Sequencing of HR k.o.
SeqPit R	GTTGATGTAAGCGCCCTCCT	
sgRNA_Alb1	AAGCTAATACGACTCACTATA GAGAATCTCGGAGACGACAGGTTTTAGAGCTAGAAATAGCAAG	sgRNA targeting *MoALB1*
sgRNA_Pit	AAGCTAATACGACTCACTATAGAGTCTTGTTATCAAGGCCAGGTTTTAGAGCTAGAAATAGCAAG	sgRNA targeting *MoPIT*
SeqAlb F	GGATTCCTCGCCGAGTTCTAC	Sequencing of *MoALB1* HR k.o.
SeqAlb R	TCGACCAGCTCACCCTAGATC	

933